Copy
RM L9E18

NACA

RESEARCH MEMORANDUM

EFFECTS OF VARIOUS OUTBOARD AND CENTRAL FINS ON LOW-SPEED STATIC-STABILITY AND ROLLING CHARACTERISTICS OF A TRIANGULAR-WING MODEL

By

Byron M. Jaquet and Jack D. Brewer

Langley Aeronautical Laboratory
Langley Air Force Base, Va.

NATIONAL ADVISORY COMMITTEE
FOR AERONAUTICS

WASHINGTON
June 29, 1949

NATIONAL ADVISORY COMMITTEE FOR AERONAUTICS

RESEARCH MEMORANDUM

EFFECTS OF VARIOUS OUTBOARD AND CENTRAL FINS ON LOW-SPEED STATIC-STABILITY AND ROLLING CHARACTERISTICS OF A TRIANGULAR-WING MODEL

By Byron M. Jaquet and Jack D. Brewer

SUMMARY

An investigation has been conducted in the 6-foot-diameter rolling-flow test section of the Langley stability tunnel to determine the effects of various outboard and central fins on the low-speed static-stability and rolling characteristics of a triangular-wing model. One of the purposes of the investigation was to determine a fin configuration which would maintain good directional stability throughout the lift-coefficient range.

Reasonably good directional stability could be obtained by the use of either outboard or central vertical fins. When the outboard arrangement was used, the most satisfactory directional stability was obtained when the fins were mounted as close to the tips as possible; the characteristic triangular-wing vortices appear to cause less adverse effects on the fin effectiveness for the extreme outboard location. The best central-fin arrangement to obtain good directional stability, along with comparatively low effective dihedral, was the high-aspect-ratio (2.31) fin mounted in the forward position (trailing edge of fin at trailing edge of wing) on the fuselage.

For either outboard or central arrangements, the fins were much more important than the wing itself in contributing to the lateral force due to roll and the yawing moment due to roll. Although the contribution of the fins to the damping in roll was smaller than the contribution of the wing, it was of significant magnitude.

INTRODUCTION

In estimating the dynamic stability of an airplane, it is necessary to know the static and rotary stability derivatives. In reference 1 it was noted that some of the stability derivatives of triangular wings could not be predicted with good or even fair accuracy by available theories. As a result, the estimation of the stability of a triangular-wing airplane would be unreliable unless an experimental means of obtaining the stability derivatives was used.

Since the original concept of the use of triangular wings for high-speed flight, numerous experimental investigations have been made to determine the low-speed static-stability characteristics and, in some cases, the damping in roll of these wings. (See references 2 and 3.) Previous investigations have been rather limited in scope since they did not provide much information on the contribution of the fuselage and various vertical-tail arrangements to the stability derivatives (particularly the rotary derivatives). The damping in roll was generally determined by the use of a forced rotation rig, such as the one described in reference 4, and, as a result, complete models could not be tested with ease.

In the Langley stability tunnel it is possible to determine experimentally the rolling, pitching, and yawing derivatives of complete models in addition to the static stability derivatives. To obtain the rolling derivatives (as in the present case) the model is mounted rigidly on a conventional balance strut and the air stream is rolled about the model by means of rotating vanes. (See reference 4.)

The present investigation was conducted to determine the effects of various centrally located vertical fins, in two positions on the fuselage, and the effects of two outboard-fin configurations, in various spanwise positions, on the low-speed static-stability and rolling characteristics of a triangular-wing model. The model selected is representative of current designs of triangular-wing aircraft.

One of the purposes of the present investigation is to attempt to determine a fin configuration which will maintain good directional stability throughout the lift-coefficient range.

SYMBOLS

The data presented herein are in the form of standard NACA coefficients of forces and moments which are referred to the stability system of axes with the origin at the calculated aerodynamic center of the wing. The positive directions of the forces, moments, and angular displacements are shown in figure 1. The coefficients used herein are defined as follows:

C_L	lift coefficient (L/qS)
$C_{L_{max}}$	maximum lift coefficient
C_X	longitudinal-force coefficient (X/qS)
C_Y	lateral-force coefficient (Y/qS)
C_l	rolling-moment coefficient (L'/qSb)
C_m	pitching-moment coefficient ($M/qS\bar{c}$)
C_n	yawing-moment coefficient (N/qSb)
L	lift, pounds
X	longitudinal force, pounds
Y	lateral force, pounds
L'	rolling moment, foot-pounds
M	pitching moment, foot-pounds
N	yawing moment, foot-pounds
A	aspect ratio $\left(b^2/S\right)$
b	span, feet
S	area, square feet
c	chord parallel to plane of symmetry, feet

$\bar{c}$ mean aerodynamic chord, feet $\left(\frac{2}{S}\int_0^{b/2} c^2 dy\right)$

x longitudinal distance from apex of triangle to quarter-chord point of any chordwise section, feet

$\bar{x}$ longitudinal distance from apex of triangle to quarter-chord point of mean aerodynamic chord, feet $\left(\frac{2}{S}\int_0^{b/2} cx\ dy\right)$

λ taper ratio

R Reynolds number

q dynamic pressure, pounds per square foot $\left(\rho V^2/2\right)$

ρ density of air, slugs per cubic foot

V free-stream velocity, feet per second

α angle of attack measured in plane of symmetry, degrees

ψ angle of yaw, degrees

Λ_{LE} angle of sweepback of leading edge, degrees

$\Lambda_{c/4}$ angle of sweepback of quarter-chord line, degrees

$pb/2V$ helix angle generated by wing tip in roll, radians

p angular velocity in roll, radians per second

$C_{L_\alpha} = \frac{\partial C_L}{\partial \alpha}$

$C_{l_\psi} = \frac{\partial C_l}{\partial \psi}$

$C_{n_\psi} = \frac{\partial C_n}{\partial \psi}$

$$C_{Y_\psi} = \frac{\partial C_Y}{\partial \psi}$$

$$C_{l_p} = \frac{\partial C_l}{\partial \frac{pb}{2V}}$$

$$C_{n_p} = \frac{\partial C_n}{\partial \frac{pb}{2V}}$$

$$C_{Y_p} = \frac{\partial C_Y}{\partial \frac{pb}{2V}}$$

Subscripts:

w wing

t fin

APPARATUS, MODEL, AND TESTS

The present investigation was conducted in the 6-foot-diameter rolling-flow test section of the Langley stability tunnel which is described in reference 4. The tests were made on a conventional six-component balance system with the model mounted at the calculated aerodynamic center of the wing.

All of the component parts of the model were constructed of laminated mahogany and were given highly polished surfaces. The wing had an angle of sweepback of the leading edge of 60°, a modified NACA $65_{(06)}$-006.5 profile parallel to the plane of symmetry, and an aspect ratio of 2.31. The ordinates of the fuselage are given in table I. The fuselage cross section was circular. A slot was cut in the top of the fuselage to allow forward and rearward movement of the central vertical fins. The pertinent dimensions of the wing and fuselage are shown in figure 2. Outboard fins of aspect ratio 1.5, $\Lambda_{LE} = 45°$, and $\lambda = 0.45$ were tested in the spanwise positions shown in figure 3(a). Shown in figure 3(b) are

the spanwise positions of the outboard fins of $A = 1.4$ with $\Lambda_{LE} = 53^\circ$ and $\lambda = 0.22$. Single central vertical fins having aspect ratios of 0.77, 1.15, and 2.31 were tested on the fuselage in the two positions shown in figure 4. The fins of $A = 0.77$ and $A = 1.15$ were previously tested on a triangular wing without a fuselage and are reported in reference 1. Photographs of some of the models are presented as figures 5 to 10.

To obtain the aerodynamic characteristics of the model at $\psi = 0^\circ$, measurements were made of the lift, longitudinal force, and pitching moment through an angle-of-attack range from about $\alpha = -4^\circ$ to $\alpha = 38^\circ$. The model was tested through the same angle-of-attack range at $\psi = \pm 5^\circ$ to determine the static-stability derivatives C_{l_ψ}, C_{n_ψ}, and C_{Y_ψ} for each fin configuration. The rolling moment, yawing moment, and lateral force were measured through a yaw range of -30° to 30° at angles of attack of about 0°, 6°, 12°, 18°, 24°, and 30°. The rolling derivatives were determined for each fin configuration by testing the model through the angle-of-attack range at values of $pb/2V$ of -0.066, -0.020, 0.023, and 0.071. The test Reynolds number and Mach number were 1.624×10^6 and 0.13, respectively.

CORRECTIONS AND ACCURACY

The angle of attack, the longitudinal-force coefficient, and the rolling-moment coefficient were corrected for the effects of the jet boundaries. The data are not corrected for blocking.

In rolling flow the support tares appeared negligible for the wing alone up to approximately $\alpha = 16^\circ$. However, at higher angles of attack there were large interference effects, and, since they could not be accurately evaluated, the rolling derivatives above approximately $\alpha = 16^\circ$ are not presented.

The measurements taken are believed to be accurate within the following limits:

α, degrees	±0.1
ψ, degrees	±0.1
C_L	±0.0025
C_X	±0.0025
C_Y	±0.0005
C_l	±0.00047
C_m	±0.0011
C_n	±0.00042

RESULTS AND DISCUSSION

Presentation of Results

In presenting the data of the present paper, the various outboard fins and central fins are considered to be component parts of one model. In some of the plots the wing–fuselage–combination data are included so that the contribution of each fin can be seen more easily.

The data are presented in the following groups:

	Figures
Basic wing and wing–fuselage combination	11 to 15
Effect of outboard fins	16 to 26
Effect of central fins	27 to 38

Some of the important stability characteristics are presented in table II (at $C_L = 0$) to enable a more direct comparison of the configurations.

Wing and Wing-Fuselage Results

The addition of a fuselage to the triangular wing slightly decreases the lift-curve slope and the value of $C_{L_{max}}$ (fig. 11). A conspicuous characteristic of the wing, also apparent when the fuselage is present, is the flat portion of the lift curve at and slightly below the maximum lift coefficient. The fuselage causes a slight decrease in longitudinal stability below $C_L = 0.2$ and an increase in longitudinal stability at higher lift coefficients.

The fuselage causes a destabilizing increment in the directional-stability parameter C_{n_ψ} and causes a slight decrease in the variation of C_{l_ψ} with C_L at $C_L = 0$ (fig. 12). The addition of the fuselage to the wing causes the curves of C_n plotted against ψ to become nonlinear at smaller lift coefficients, whereas the curves of C_l plotted against ψ are not appreciably changed (figs. 13 and 14).

The variation of C_{Y_p} with C_L is slightly decreased by the addition of the fuselage. (See fig. 15 and table II.) The fuselage adds a small positive increment to the curve of C_{n_p} for the wing which results in a more positive variation of C_{n_p} with C_L for the wing-fuselage combination. It should be noted that C_{n_p} for the wing is zero or positive at positive lift coefficients, whereas reference 1 reported that available theories predict negative values of C_{n_p} at small positive lift coefficients. The fuselage had a very small effect on C_{l_p}.

Effect of Outboard Fins

Small symmetrical outboard fins.- Mounting the fins of $A = 1.5$, $\lambda = 0.45$, and $\frac{S_t}{S_w} = 0.083$, symmetrical above and below wing chord line,

(see fig. 3(a)) in either position 1 or 2 does not produce any significant changes in C_{L_α} or longitudinal stability at low lift coefficients (fig. 16 and table II). However, when the fins are in the inboard position (position 2) a sudden decrease occurs in C_{L_α} at $C_L = 0.63$. A sudden decrease occurs in longitudinal stability at the same lift coefficient.

Tuft studies indicated that a sudden flow reversal (stalling) occurred just outboard of the fins in either position. This reversal was not shown by tuft studies of the wing-fuselage combination. Reference 5 indicated the presence of two semispan vortices on a wing of approximately triangular plan form. Pressure investigations reported in reference 6 show that the two semispan vortices are swept inward from the tips as the angle of attack is increased. It appears that when these vortices come in contact with the fins, the vortices are disturbed in such a manner as to cause a sudden stalling of the portion of the wing outboard of the fins. As the fins are moved inboard, the contact of the vortex and the fin is delayed until a higher angle of attack, but when it does occur, the adverse affect is greater since the area outboard of the fin is larger. A brief check test of the fins of $A = 1.4$ in position 3 at a Reynolds number of 2.58×10^6 indicated that the premature stall occurred at the same lift coefficient as the lower Reynolds number tests (reported herein) indicate. It seems likely that the vortex disturbances caused by the fins also result in a decrease in fin effectiveness. This effect is shown by the breaks in the static derivatives C_{Y_ψ}, C_{n_ψ}, and C_{l_ψ} shown in figure 22. The fins do not appear large enough to give good directional stability. The variation of C_{l_ψ} with C_L is not appreciably affected by the fins in either position. (See fig. 17 and table II.)

The curves of C_n and C_l plotted against ψ are linear to higher lift coefficients when the fins are in position 1 (figs. 18 and 19).

The addition of the fins in either position caused C_{Y_p}/C_L to be more positive and C_{n_p}/C_L to be more negative than for the wing-fuselage combination (fig. 20 and table II). As the fins were moved inboard there was no displacement of C_{Y_p} or C_{n_p} at $C_L = 0$. This

effect was perhaps caused by the symmetrical arrangement of the fin above and below the wing chord line. The effect of the fins on C_{l_p} was small.

Large upper-surface outboard fins.- When the larger fins $\left(A = 1.4,\ \lambda = 0.22,\ \text{and}\ \frac{S_t}{S_w} = 0.22\right)$ shown in figure 3(b) are mounted on the wing, lower values of $C_{L_{max}}$ are obtained than those obtained with the previously discussed fins. (See table II.) As in the case of the smaller fins, a premature stall occurs at $C_L = 0.6$ when the larger fins are moved inboard from the tips to position 3 and at $C_L = 0.48$ when they are moved to position 2. (See fig. 21.) When the fins are in the extreme outboard position (position 1), the premature stall was not apparent and the configuration had a resulting higher maximum lift coefficient (fig. 21).

A decrease in longitudinal stability occurs at $C_L = 0.48$ when the fins are in position 2 and at $C_L = 0.6$ when the fins are in position 3. These decreases are probably due to the disturbance of the vortices described previously; the decrease occurs at a lower lift coefficient with the fins in position 2 since the fins are closer to the tips and to the leading edge of the wing in this position than in position 3. When the fins are in position 1, a sudden decrease in longitudinal stability does not occur.

Sharp breaks occur in the static derivatives C_{Y_ψ}, C_{n_ψ}, and C_{l_ψ} where the premature stall occurs (fig. 22). When the fins are in the extreme outboard position (position 1), good directional stability is obtained almost to $C_{L_{max}}$. It seems apparent that, for a triangular-wing configuration using outboard fins, the best directional stability is obtained when the fins are located as close to the wing tips as is possible; the vortices appear to cause less adverse effects on the fin effectiveness for the extreme outboard location. As the fins are moved inboard, the variation of C_{l_ψ} with C_L is slightly decreased, as are the values of C_{l_ψ} at $C_L = 0$ (fig. 22 and table II).

More linear curves of C_l and C_n plotted against ψ are obtained when the fins are in position 1 (figs. 23, 24, and 25) than either of the other positions.

Moving the fins inboard from the tips does not appreciably affect C_{Y_p}/C_L, but the values of C_{Y_p} at $C_L = 0$ become less negative (fig. 26 and table II). All three positions give larger variations of C_{Y_p} with C_L than the wing-fuselage combination. In general, moving the fins inboard results in a less negative variation of C_{n_p} with C_L (which is of opposite sign of that of the wing-fuselage combination) and less positive values of C_{n_p} at $C_L = 0$. Moving the fins inboard from the tips causes a decrease in C_{l_p} at $C_L = 0$. In general, C_{l_p} decreases slightly with an increase in lift coefficient. A sharp decrease occurs in C_{l_p} at the lift coefficient corresponding to the premature stall (fig. 26).

It appears that, if good directional stability is desired, outboard fins may be used on a triangular-wing airplane only if they are mounted as close to the tips as is possible; the vortices seem to cause less adverse effects on the fin effectiveness for the extreme outboard location.

Effect of Central Fins

Forward position.- The central vertical fins had very small effects on the lift, longitudinal-force, and pitching-moment characteristics of the model as is seen in figure 27 and table II.

Increasing the fin aspect ratio results in an increase in directional stability up to $C_{L_{max}}$ (fig. 28). The fins of $A = 1.15$ and $A = 2.31$ provide smaller variations of C_{l_ψ} with C_L than the other fin (fig. 28 and table II). The use of negative dihedral would probably shift the curve of C_{l_ψ} down to a smaller maximum value.

It appears that the fin of $A = 2.31$ would be more satisfactory than either of the others, since it provides good directional

stability up to $C_{L_{max}}$ (fig. 28) and generally good directional stability through the yaw range (fig. 31). The effective dihedral for this fin configuration is not very large.

In general, as the fin aspect ratio is increased C_{Y_p} is displaced negatively, C_{n_p} is displaced positively, and C_{l_p} is increased at $C_L = 0$ (fig. 32 and table II). The variations of C_{Y_p} and C_{n_p} with C_L are increased and decreased, respectively, as the fin aspect ratio is increased. Decreased damping in roll is noted for all configurations as the lift coefficient is increased.

A comparison of figures 26 and 32 shows that the effect of the outboard fins is greater than the effect of the central fins on C_{n_p}; the values of C_{n_p} for the outboard fins change sign, whereas C_{n_p} for the central fins varies only slightly with an increase in C_L.

It should be noted that the contribution of the fins to C_{Y_p} and C_{n_p} is much greater than the contribution of the wing. Although the contribution of the fins to C_{l_p} is smaller than the contribution of the wing, it is of significant magnitude.

Rearward position.- When the fins are moved to the rearward position, higher values of $C_{L_{max}}$ are obtained. (Compare figs. 27 and 33.) The longitudinal stability at $C_L = 0$ is not appreciably changed by moving the fins from the forward to the rearward position on the fuselage (table II).

Good directional stability is obtained with each of the fins, except near maximum lift coefficient where sudden unstable changes occur. (See fig. 34.) The variation of C_{l_ψ} with C_L decreases as the fin aspect ratio is increased, the fin of $A = 1.15$ providing the smallest variation as it did in the forward position.

In general, more linear curves of C_Y, C_n, and C_l plotted against ψ are obtained with the fin of $A = 2.31$. (Compare figs. 35, 36, and 37.)

The forward position on the fuselage appears to be the superior position since smaller values of effective dihedral are obtained along with good directional stability up to $C_{L_{max}}$ (for the fin of A = 2.31), whereas in the rearward position the directional stability changes suddenly at $C_{L_{max}}$ from stable to unstable values.

In the rearward position the effects of the fins on the rolling derivatives were similar, although larger in magnitude, to the effects noted for the forward position. (Compare figs. 32 and 38.)

CONCLUSIONS

An investigation of the low-speed static-stability and rolling characteristics of a triangular-wing model with various fin arrangements indicates the following conclusions:

1. Reasonably good directional stability can be obtained by the use of either outboard or central vertical fins.

2. When the outboard arrangement was used, the most satisfactory directional stability was obtained when the fins were mounted as close to the tips as possible; the characteristic triangular wing vortices appear to cause less adverse effects on the fin effectiveness for the extreme outboard location.

3. The best central-fin arrangement to obtain good directional stability, along with comparatively low effective dihedral, was the high-aspect-ratio (A = 2.31) fin mounted in the forward position (trailing edge of fin at trailing edge of wing) on the fuselage.

4. For either outboard or central arrangements, the fins were much more important than the wing itself in contributing to the lateral force due to roll and the yawing moment due to roll. Although the contribution of the fins to the damping in roll was smaller than the contribution of the wing, it was of significant magnitude.

Langley Aeronautical Laboratory
National Advisory Committee for Aeronautics
Langley Air Force Base, Va.

REFERENCES

1. Jaquet, Byron M., and Brewer, Jack D.: Low-Speed Static-Stability and Rolling Characteristics of Low-Aspect-Ratio Wings of Triangular and Modified Triangular Plan Forms. NACA RM L8L29, 1949.

2. Tosti, Louis P.: Low-Speed Static Stability and Damping-in-Roll Characteristics of Some Swept and Unswept Low-Aspect-Ratio Wings. NACA TN 1468, 1947.

3. McKinney, Marion O., Jr., and Drake, Hubert M.: Flight Characteristics at Low Speed of Delta-Wing Models. NACA RM L7K07, 1948.

4. MacLachlan, Robert, and Letko, William: Correlation of Two Experimental Methods of Determining the Rolling Characteristics of Unswept Wings. NACA TN 1309, 1947.

5. Wilson, Herbert A., Jr., and Lovell, J. Calvin: Full-Scale Investigation of the Maximum Lift and Flow Characteristics of an Airplane Having Approximately Triangular Plan Form. NACA RM L6K20, 1947.

6. Anderson, Adrien E.: Chordwise and Spanwise Loadings Measured at Low Speed on Large Triangular Wings. NACA RM A9B17, 1949.

TABLE I

Ordinates of fuselage.

Station	x, in.	y, in.
1	0	0
2	.02	.20
3	.09	.40
4	.38	.80
5	.62	1.00
6	.93	1.20
7	1.34	1.40
8	1.86	1.60
9	2.51	1.80
10	3.34	2.00
11	4.37	2.20
12	5.67	2.41
13	7.31	2.63
14	9.34	2.85
15	10.55	2.98
16	11.90	3.10
17	13.41	3.20
18	15.10	3.23
19	16.00	3.25
20	32.00	3.25
21	33.00	3.24
22	34.00	3.20
23	35.00	3.14
24	36.00	3.05
25	37.00	2.94
26	38.00	2.81
27	39.00	2.65
28	40.00	2.46
29	41.00	2.25
30	42.00	2.01
31	43.00	1.75
32	44.00	1.46
33	45.00	1.13
34	46.00	.79
35	46.50	.60
36	47.00	.41
37	47.50	.21
38	47.75	.11
39	48.00	0

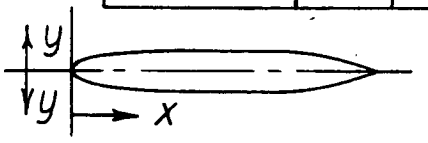

TABLE II

Summary of pertinent stability characteristics of a triangular-wing model with various vertical-fin arrangements. (All derivatives and slopes of derivatives taken at $C_L = 0$.)

Configuration	C_{L_α}	$C_{L_{max}}$	a.c. (% $\bar{c}$)	C_{l_ψ}	C_{l_ψ}/C_L	C_{n_ψ}	C_{Y_ψ}	C_{l_p}	C_{n_p}	C_{n_p}/C_L	C_{Y_p}	C_{Y_p}/C_L
Wing	.045	1.26	40.7	.0002	.0048	0	.0005	-.180	0	0	.025	.45
Wing and fuselage	.043	1.15	38.4	.0002	.0044	.0009	.0012	-.170	.011	.037	.030	.40
At 1.5 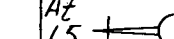 S_t/S_w .083	.043	1.10	39.5	.0002	.0043	.0001	.0043	-.178	.005	-.120	.040	.68
1.5 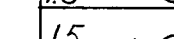 .083	.043	1.08	39.5	.0002	.0040	.0002	.0039	-.172	.010	-.055	.030	.56
1.4 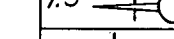 .22	.044	1.01	38.5	.0013	.0030	-.0026	.0109	-.187	.082	-.135	-.090	.70
1.4 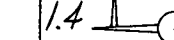 .22	.042	.95	38.5	.0010	.0029	-.0026	.0110	-.180	.058	-.040	-.060	.77
1.4 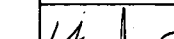 .22	.040	.95	38.5	.0008	.0028	-.0027	.0111	-.180	.026	-.075	-.030	.75
0.77 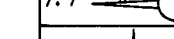 .33	.043	1.10	38.8	.0005	.0029	-.0004	.0121	-.188	.015	-.090	-.010	.71
1.15 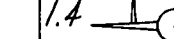 .50	.043	1.08	38.8	.0026	.0016	-.0010	.0223	-.222	.052	-.080	-.250	.92
2.31 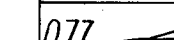 .25	.043	1.13	39.0	.0017	.0021	-.0025	.0162	-.212	.061	-.062	-.150	.79
0.77 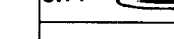 .33	.043	1.18	38.5	.0009	.0032	-.0021	.0105	-.175	.018	-.090	.030	.74
1.15 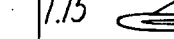 .50	.043	1.14	38.8	.0028	.0008	-.0050	.0205	-.228	.098	-.167	-.175	.97
2.31 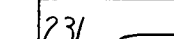 .25	.043	1.17	38.8	.0021	.0017	-.0048	.0142	-.210	.075	-.142	-.085	.93

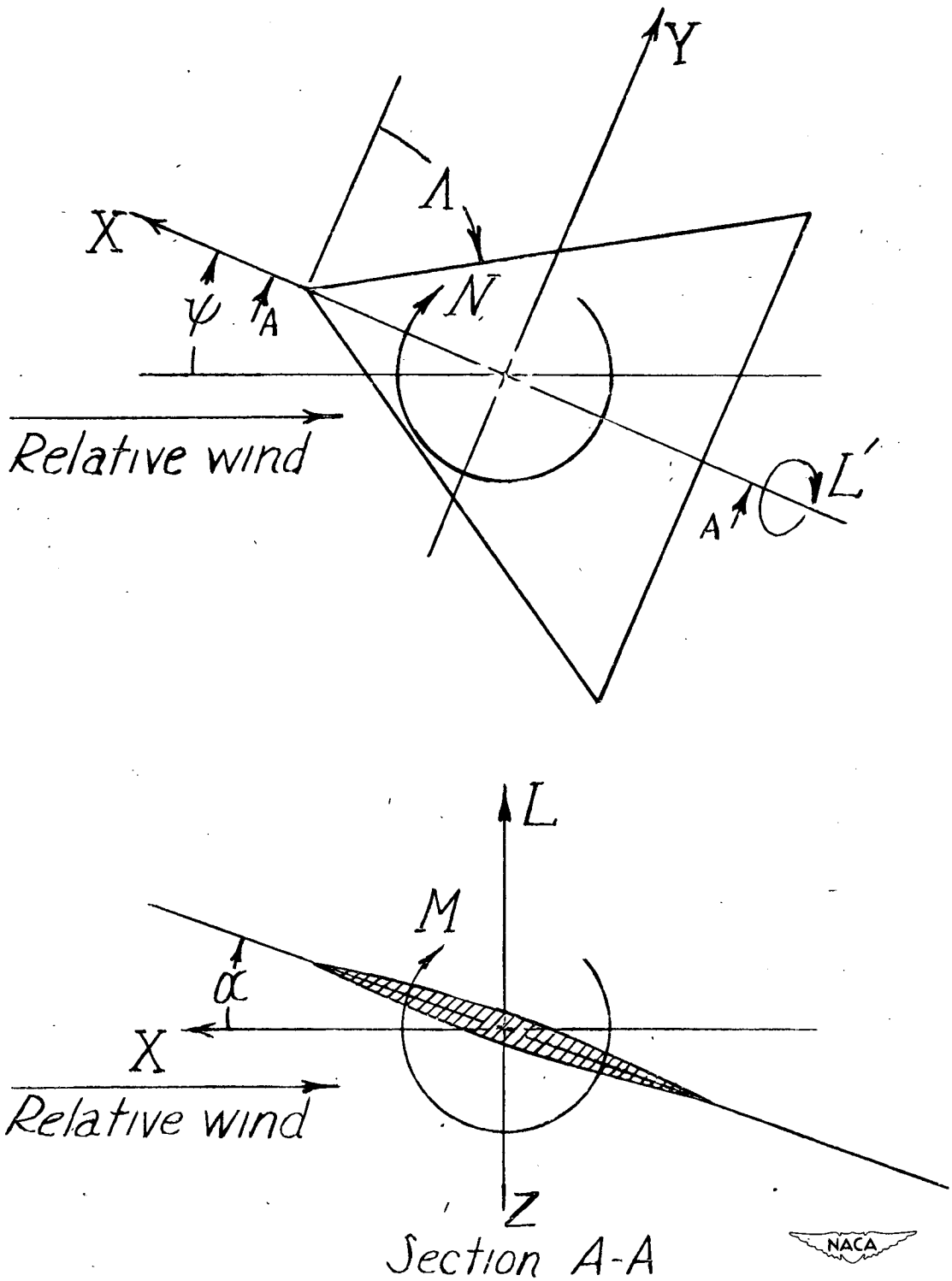

Figure 1.- System of stability axes. Positive forces, moments, and angles are indicated.

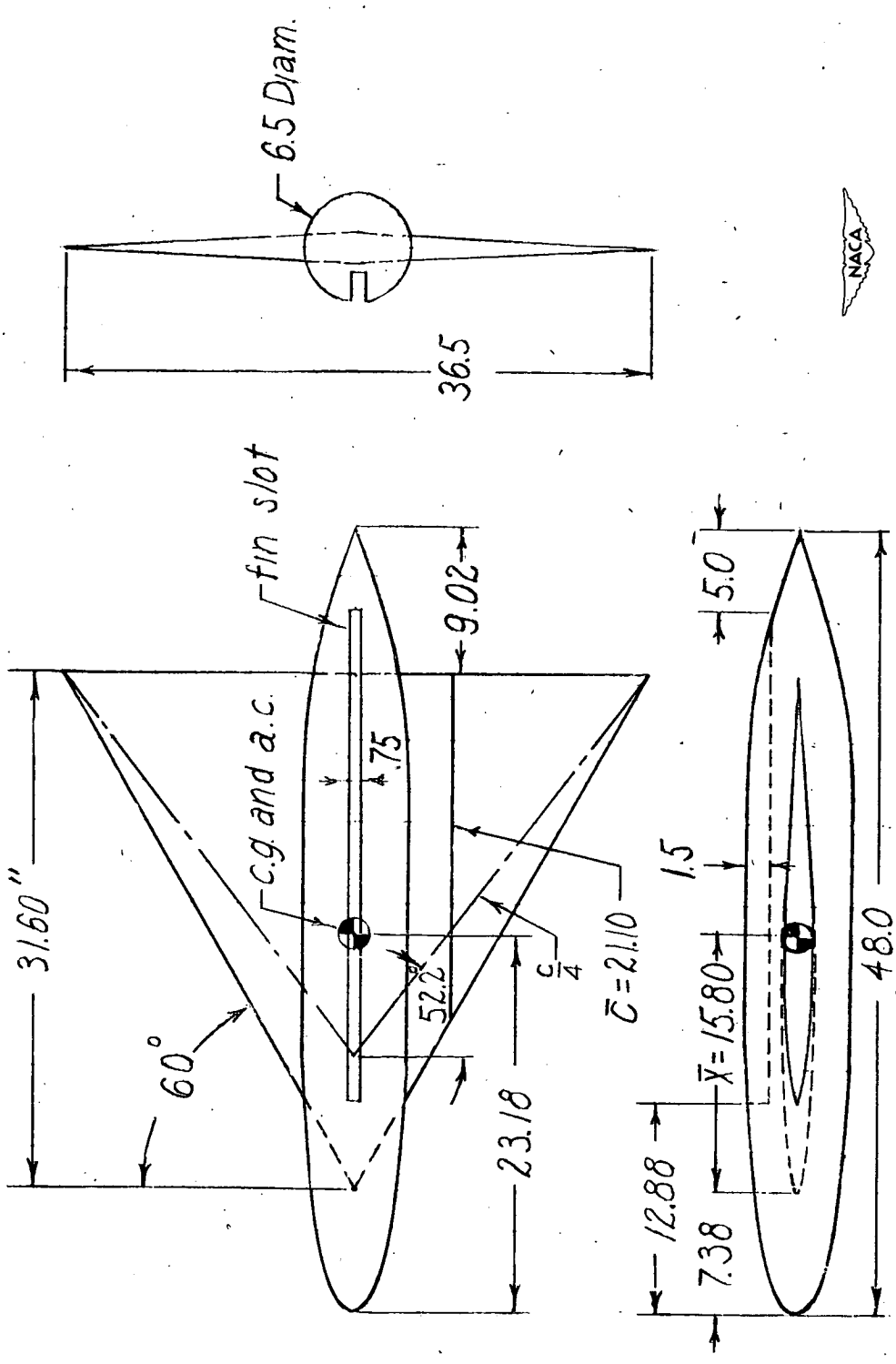

Figure 2.- Fuselage and wing details. Fineness ratio of fuselage, 7.38; wing aspect ratio, 2.31; airfoil section, modified NACA 65(06)-006.5 parallel to plane of symmetry. (All dimensions in inches.)

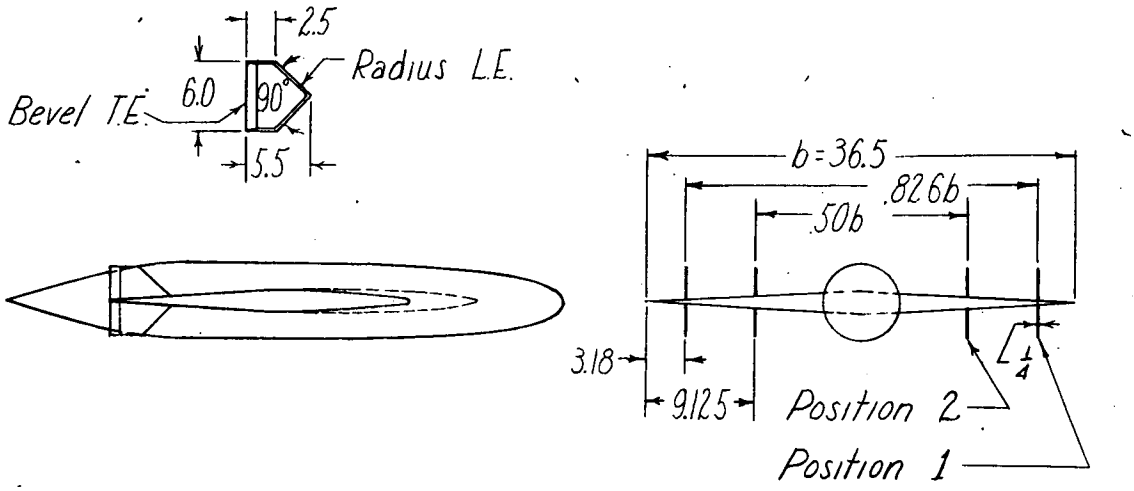

(a) $A = 1.5$; $\lambda = 0.45$; $S_t/S_W = 0.083$.

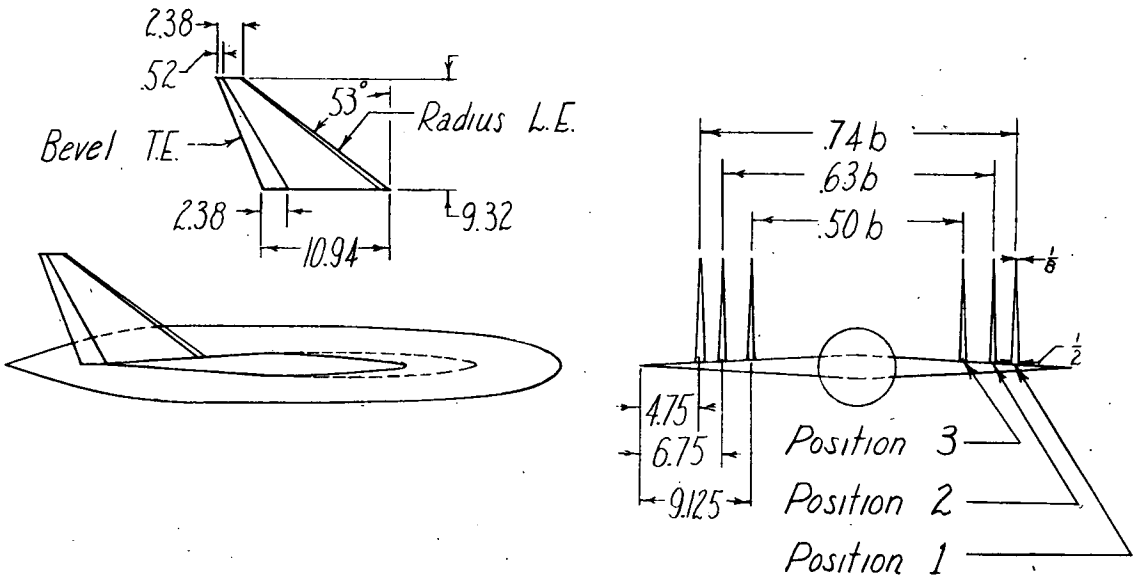

(b) $A = 1.4$; $\lambda = 0.22$; $S_t/S_W = 0.22$.

Figure 3.– Positions and dimensions of the outboard fins. All dimensions are in inches unless otherwise specified. Profile of fins, flat plate.

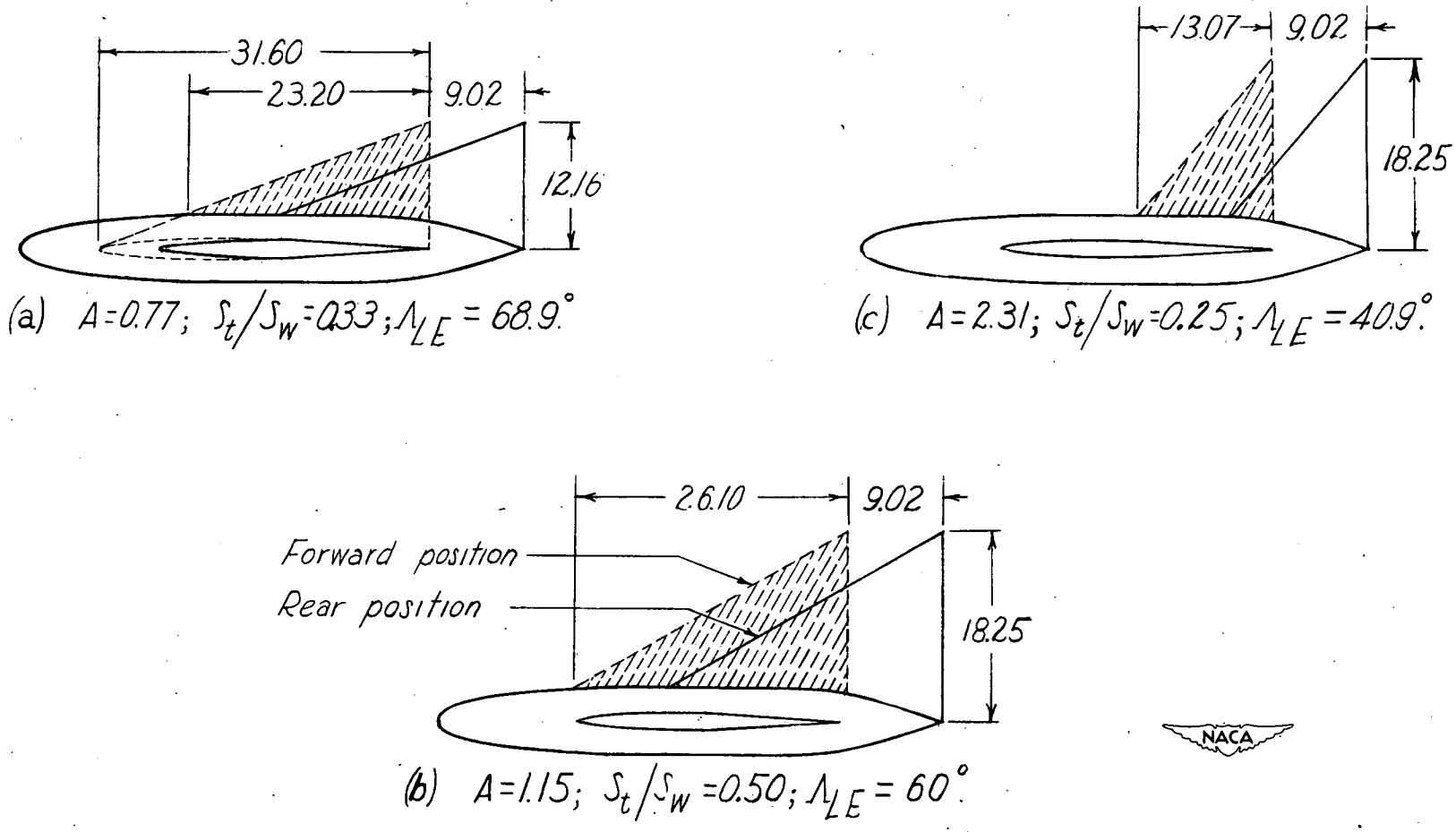

Figure 4.— Positions and dimensions of the centrally located vertical fins. All dimensions are in inches.

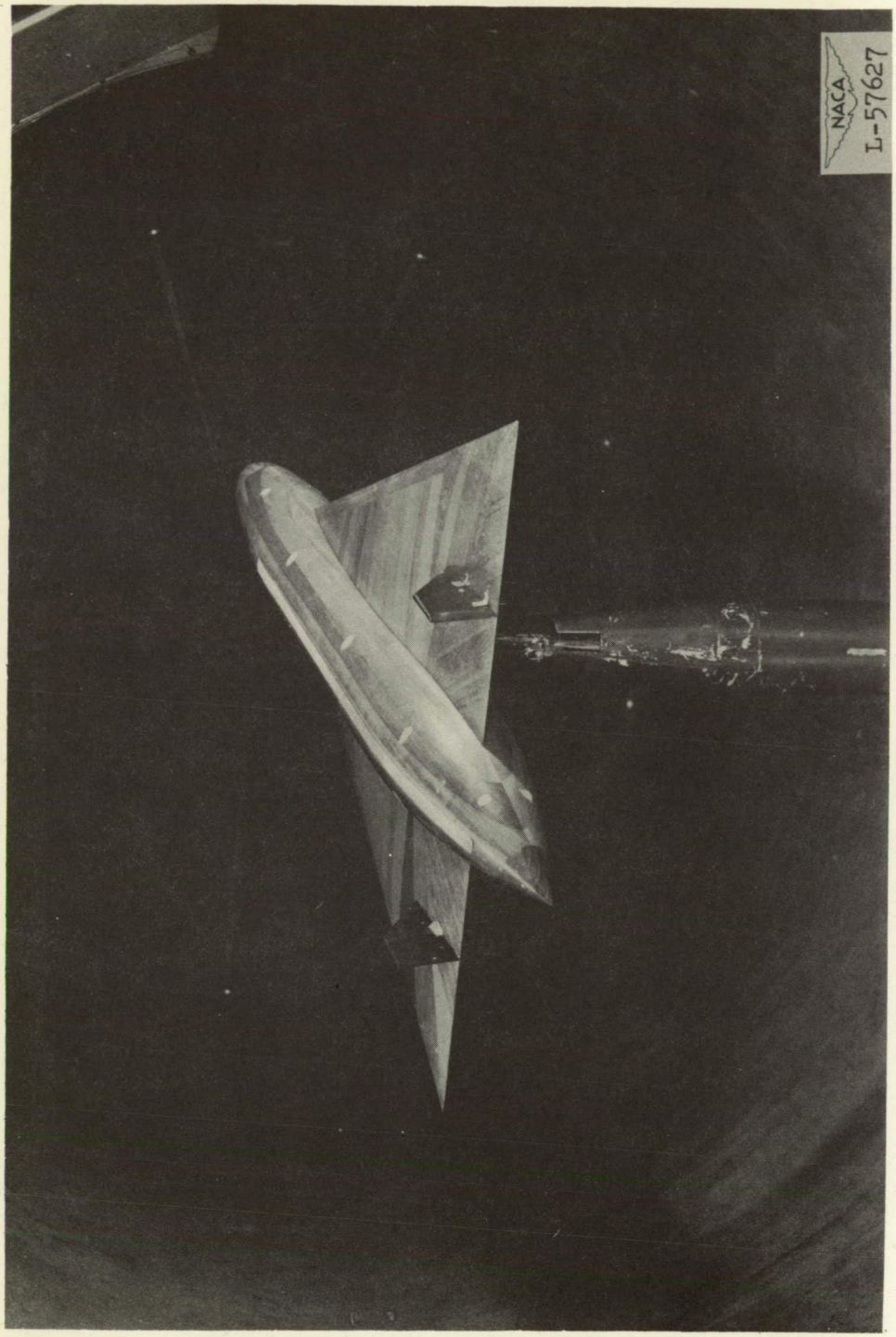

Figure 5.- Triangular-wing model with outboard fins of A = 1.5 in position 2. $\frac{S_t}{S_w} = 0.083$.

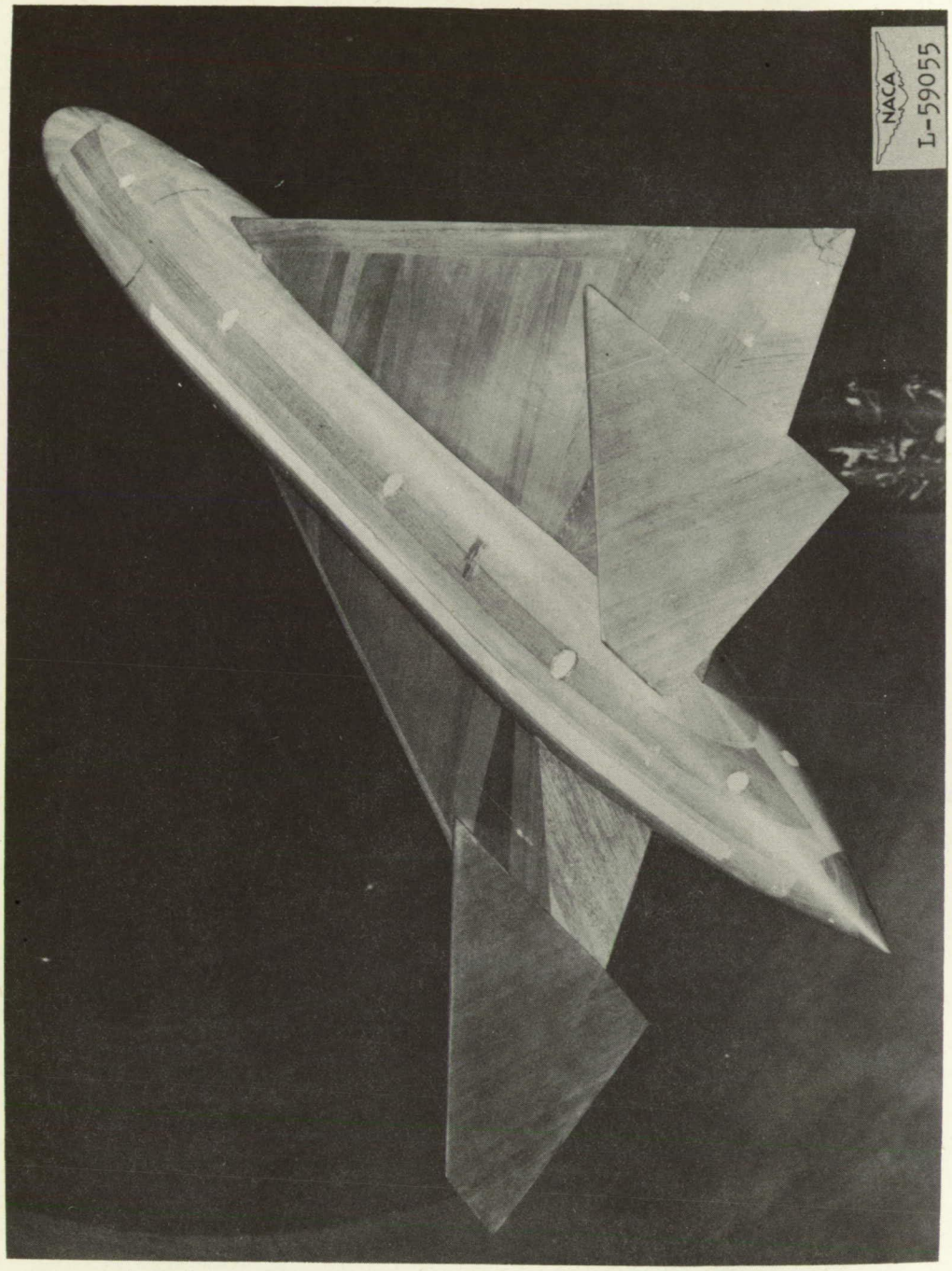

Figure 6.- Triangular-wing model with outboard fins of A = 1.4 in position 2. $\frac{S_t}{S_w} = 0.22$.

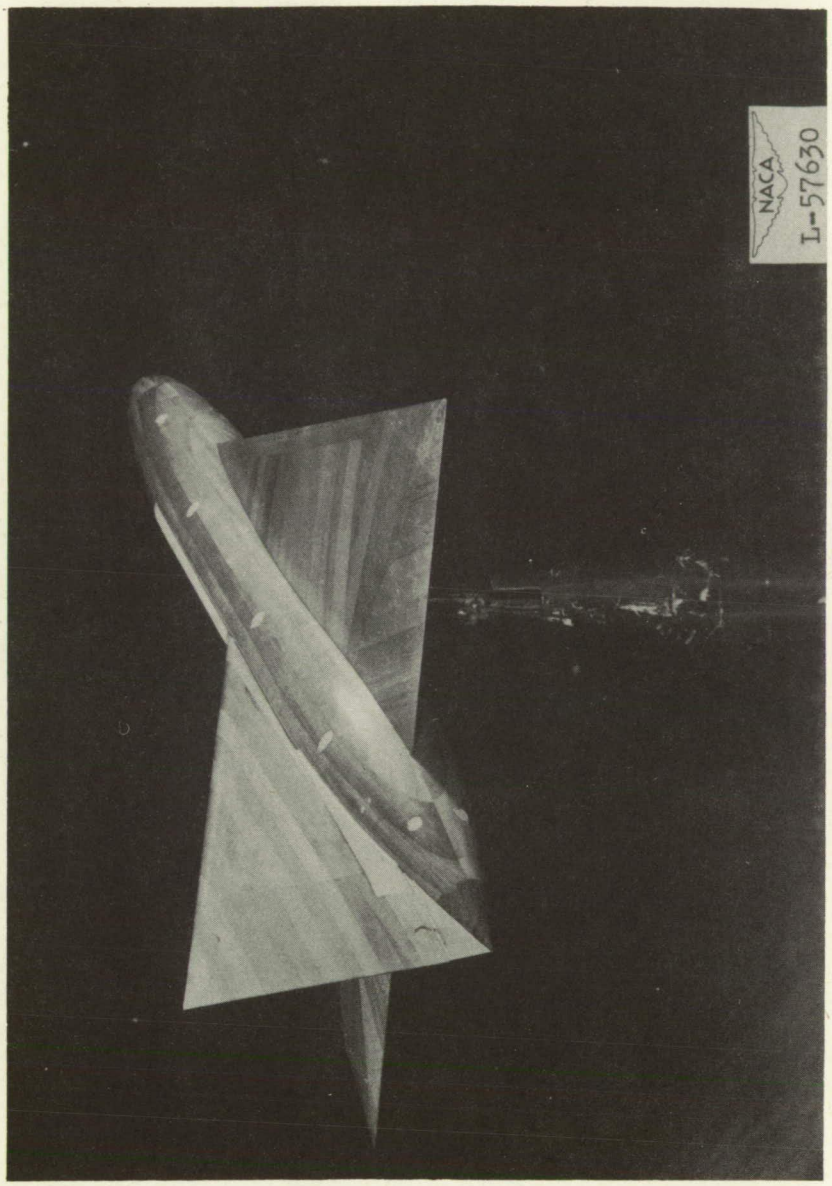

Figure 7.- Triangular-wing model with central vertical fin of A = 0.77 in rear position on fuselage. $\frac{S_t}{S_w} = 0.33$.

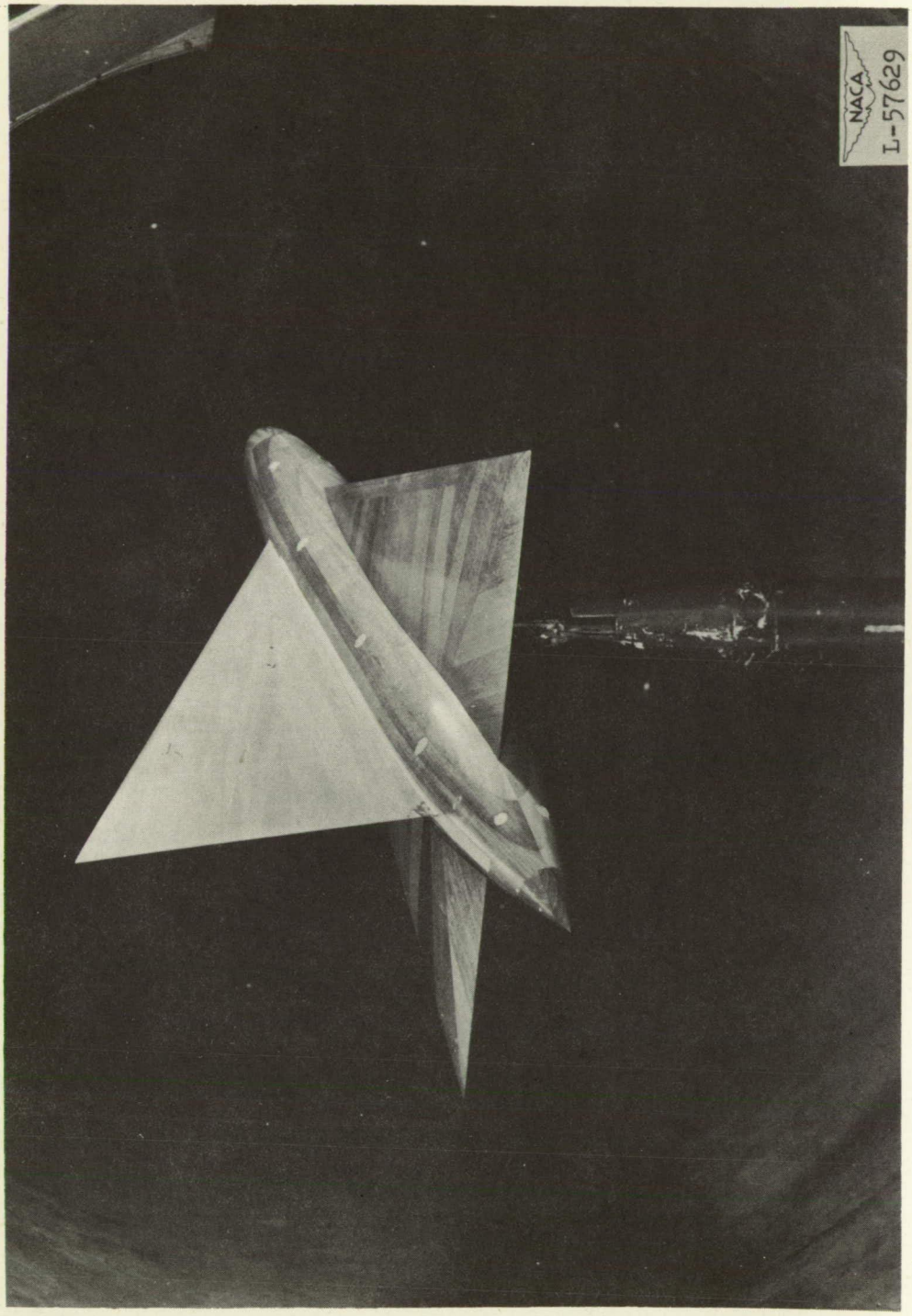

Figure 8.- Triangular-wing model with central vertical fin of A = 1.15 in forward position. $\frac{S_t}{S_w} = 0.50$.

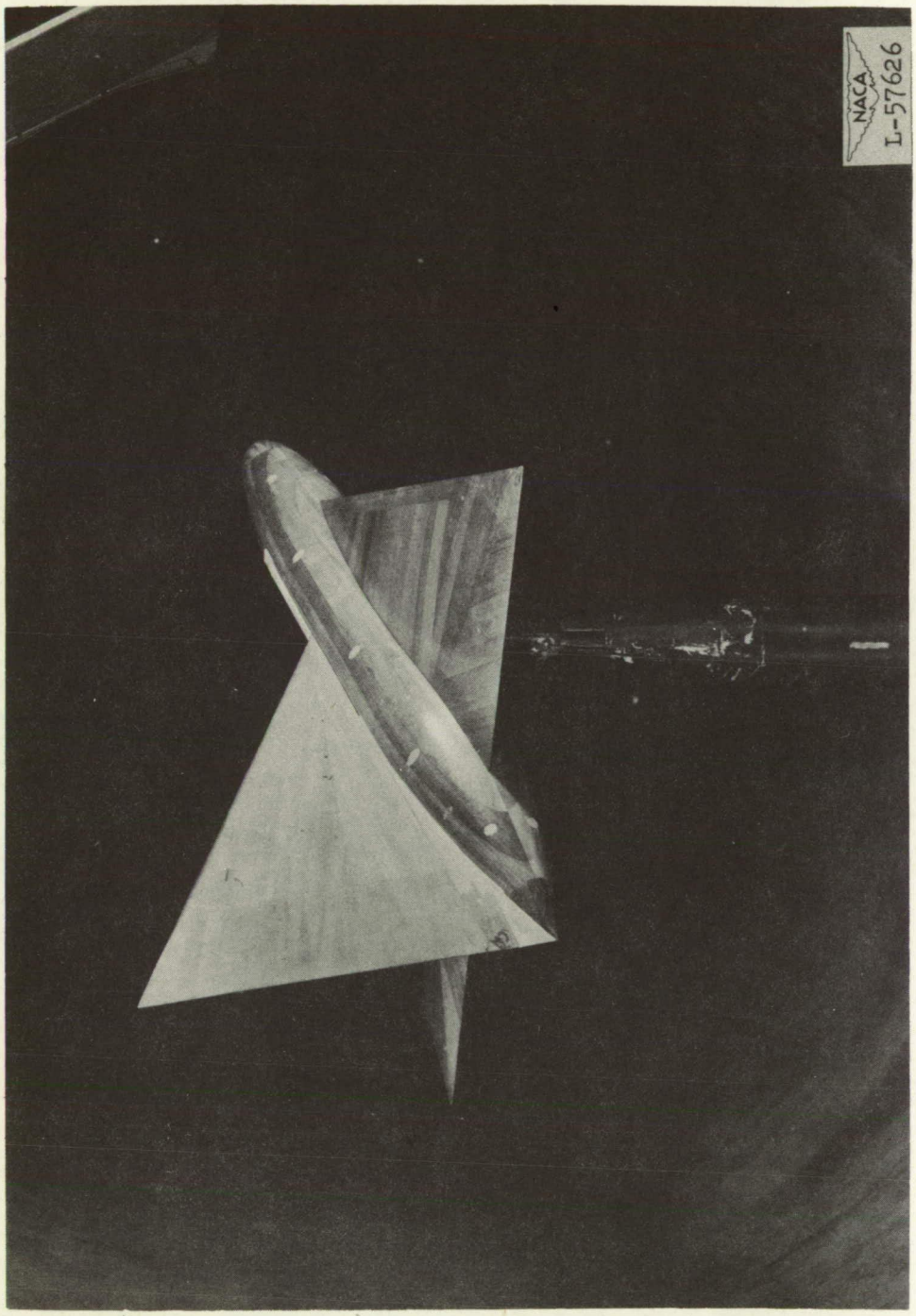

Figure 9.- Triangular-wing model with central vertical fin of A = 1.15 in rear position on fuselage. $\frac{S_t}{S_w} = 0.50$.

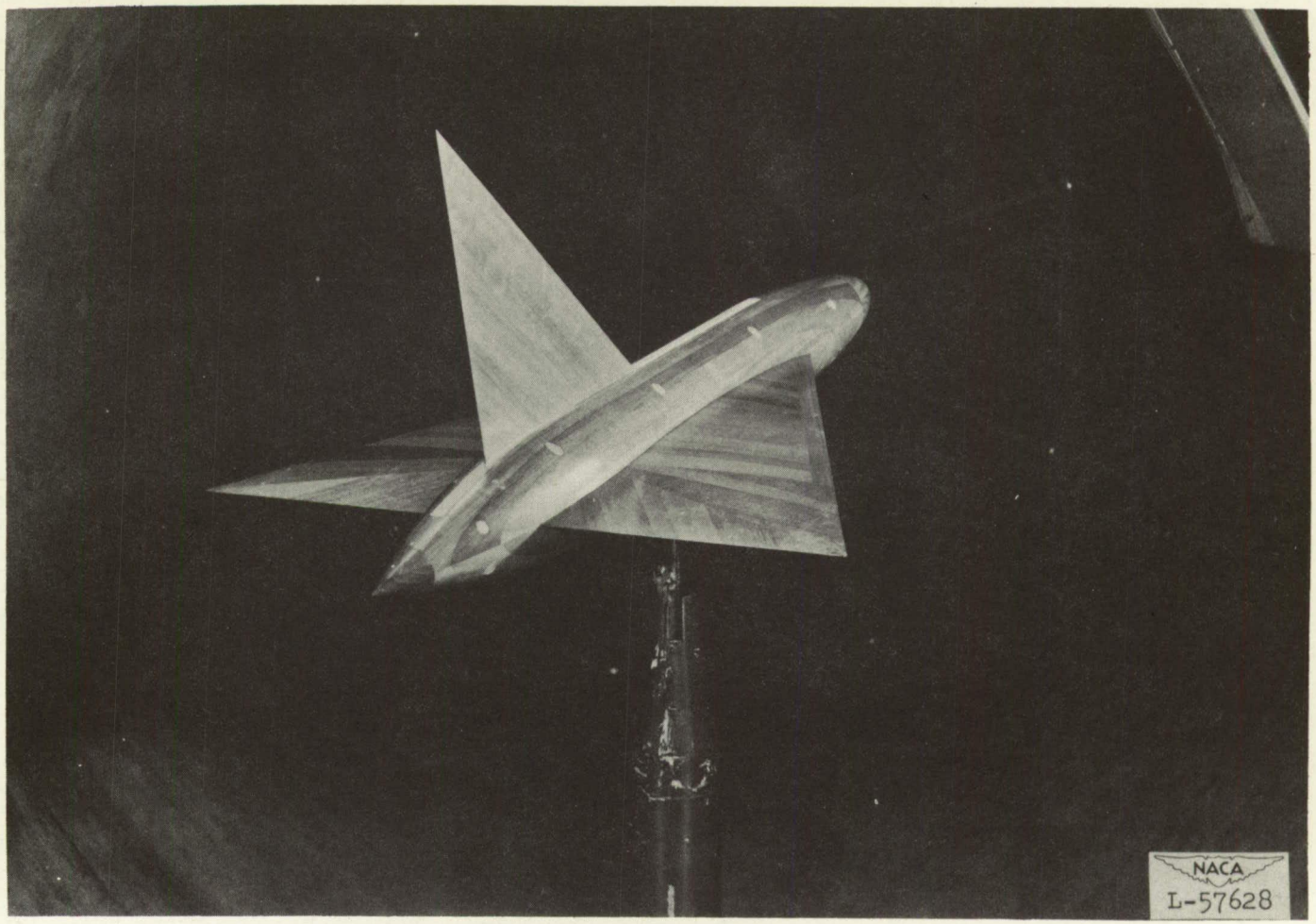

Figure 10.– Triangular-wing model with central vertical fin of $A = 2.31$ in forward position on fuselage. $\frac{S_t}{S_w} = 0.25$.

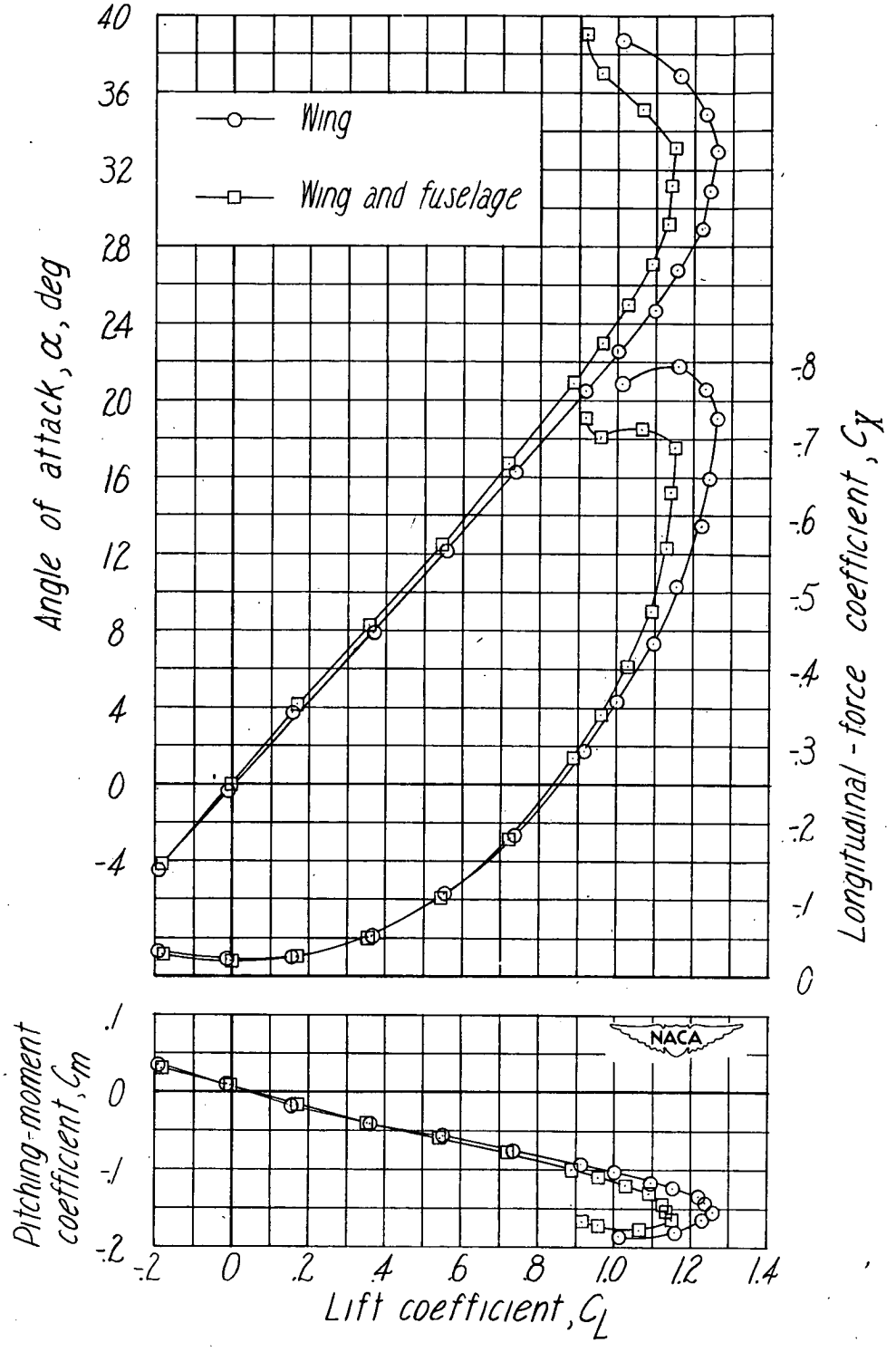

Figure 11.– Aerodynamic characteristics of a triangular wing of aspect ratio 2.31 with and without a fuselage of fineness ratio 7.38. $\Lambda_{c/4} = 52.2^{\circ}$.

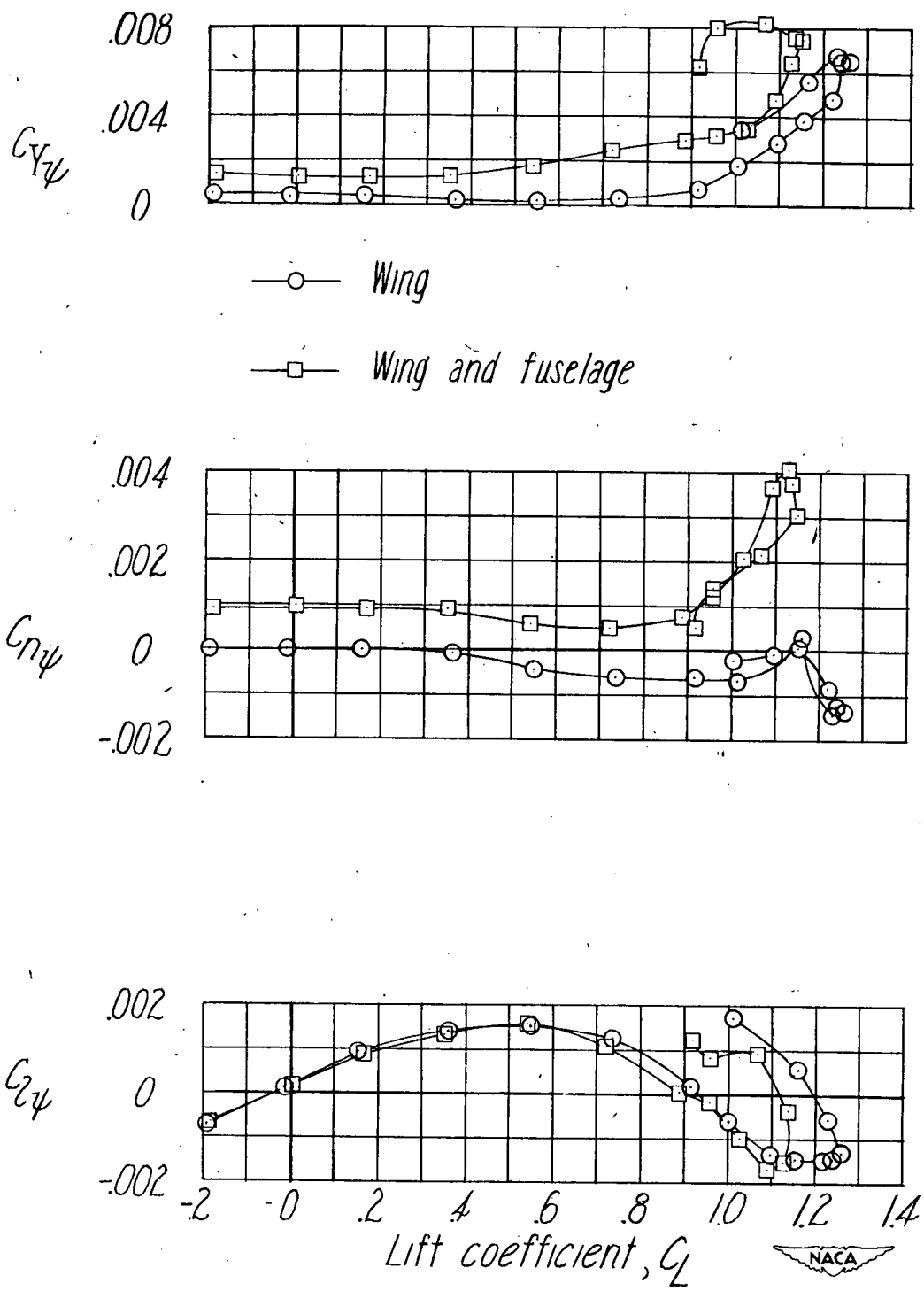

Figure 12.– Variation of C_{Y_ψ}, C_{n_ψ}, and C_{l_ψ} with C_L for a triangular wing of aspect ratio 2.31 with and without a fuselage of fineness ratio 7.38. $\Lambda_{c/4} = 52.2^\circ$.

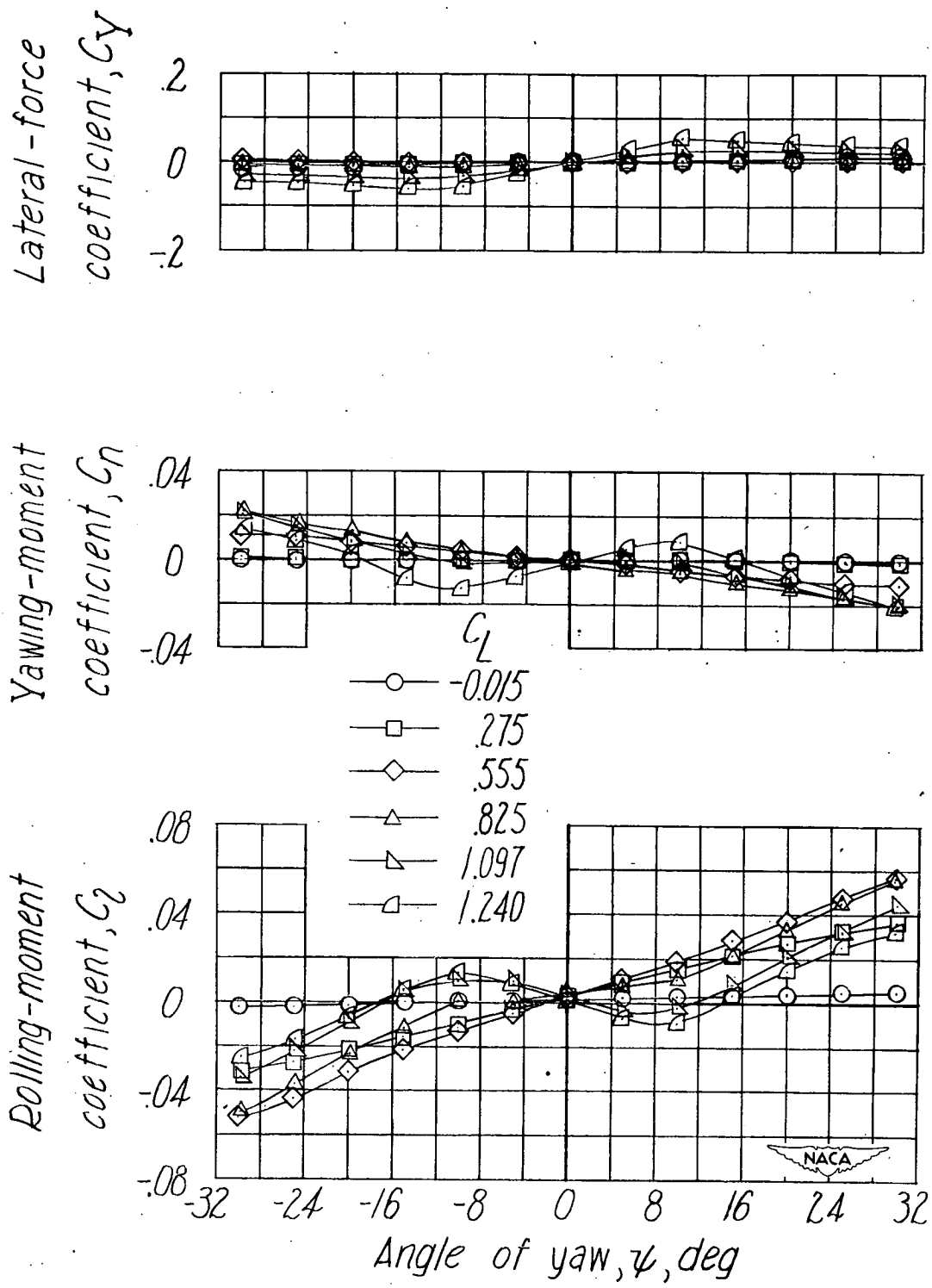

Figure 13.- Variation of C_Y, C_n, and C_l with ψ for several lift coefficients for a triangular wing of aspect ratio 2.31. $\Lambda_{c/4} = 52.2^\circ$.

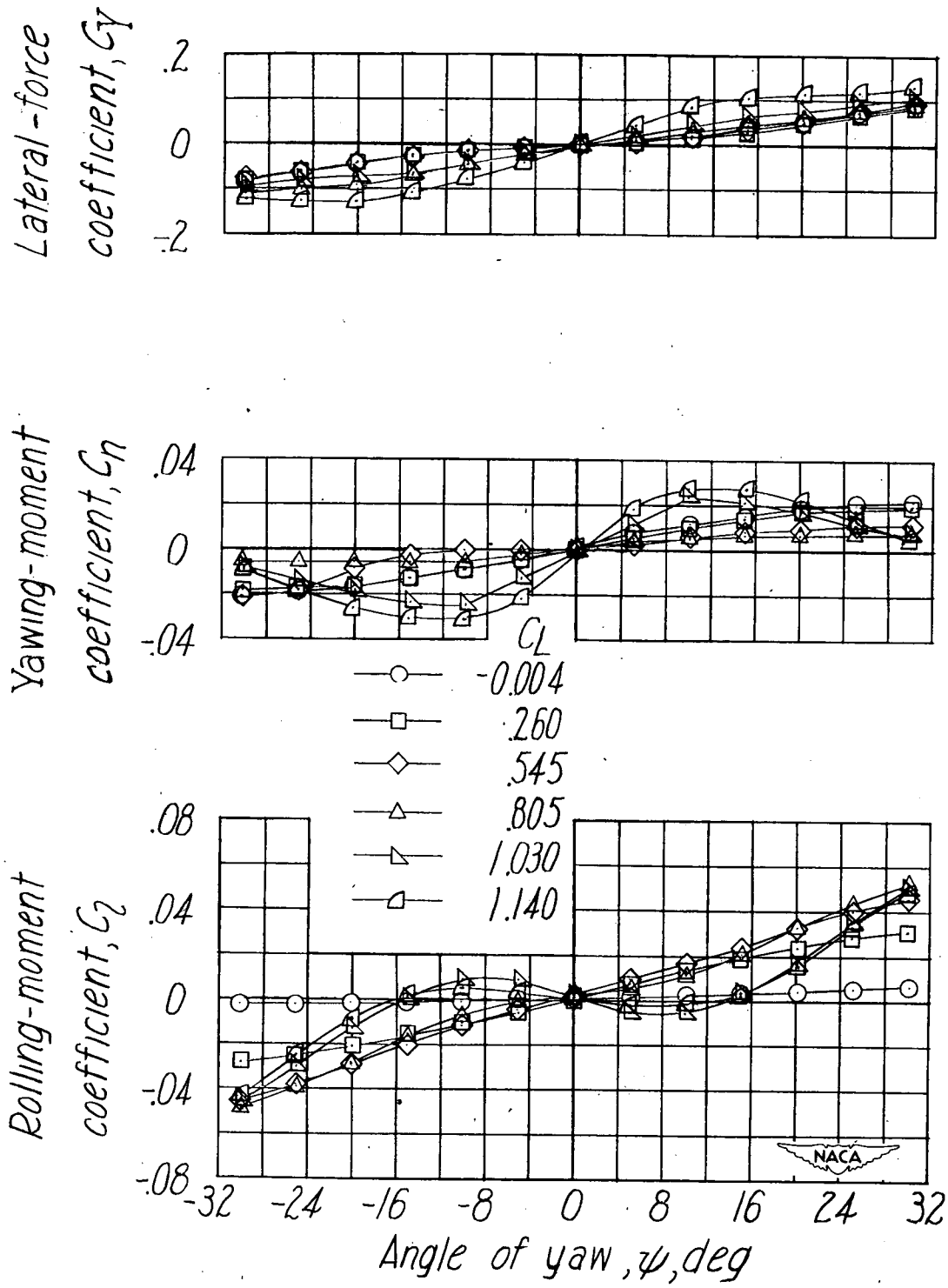

Figure 14.— Variation of C_Y, C_n, and C_l with ψ for several lift coefficients for a triangular wing of aspect ratio 2.31 with a fuselage of fineness ratio 7.38.

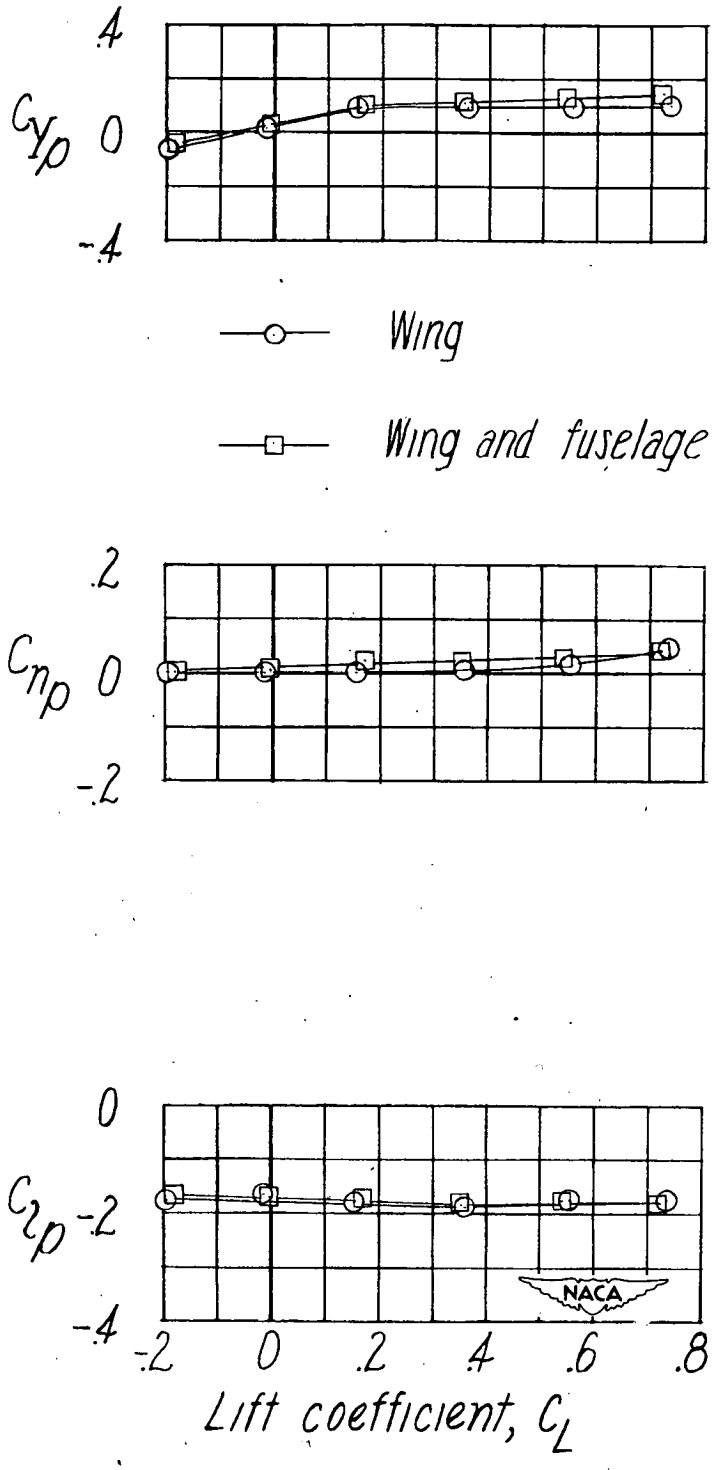

Figure 15.- Variation of C_{Y_p}, C_{n_p}, and C_{l_p} with C_L for a triangular wing of aspect ratio 2.31 with and without a fuselage of fineness ratio 7.38.

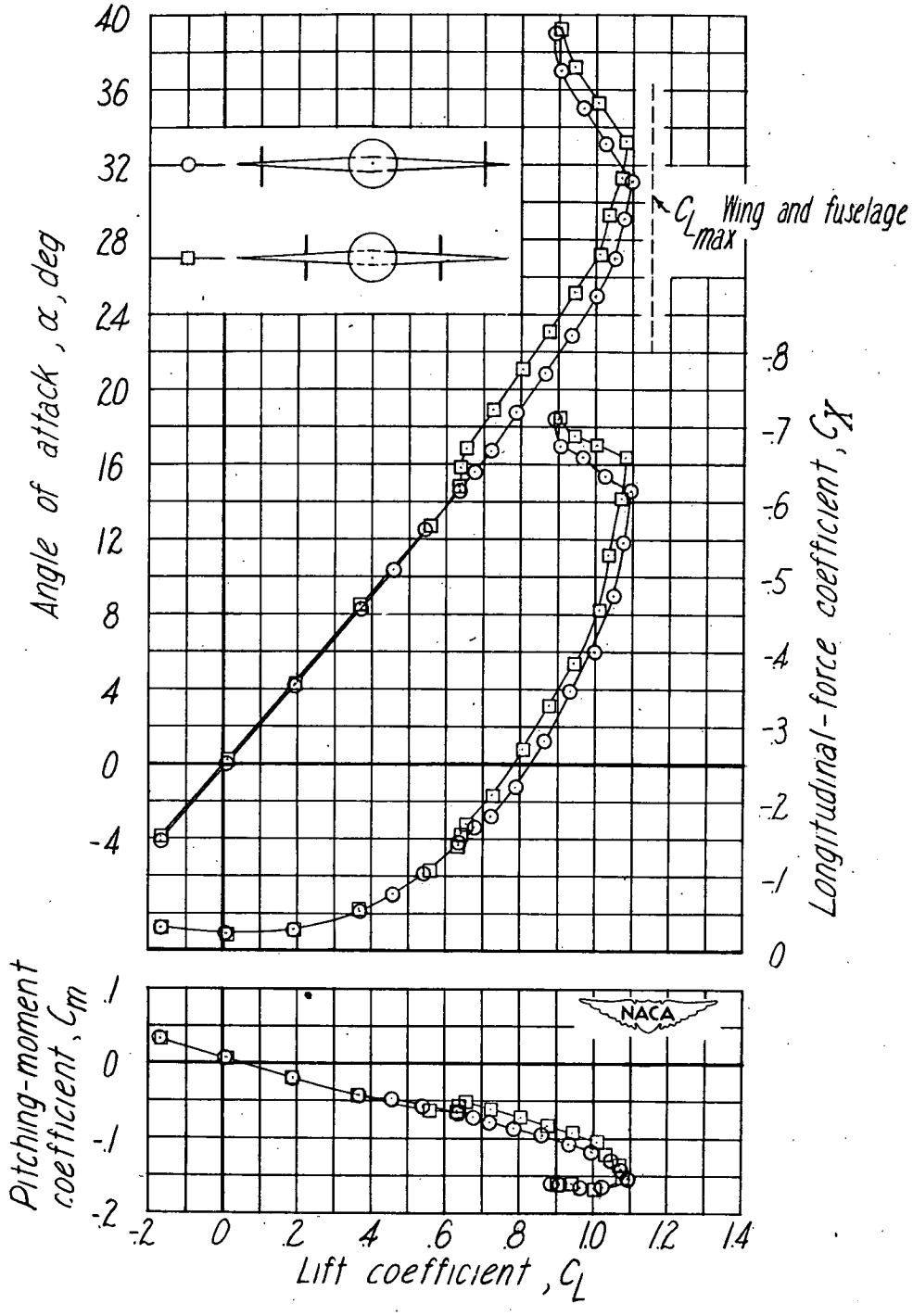

Figure 16.– Effect of outboard fin position on aerodynamic characteristics of a triangular-wing model. Fin aspect ratio, 1.5; $\Lambda_{LE} = 45°$; $\lambda = 0.45$; $\frac{S_t}{S_w} = 0.083$.

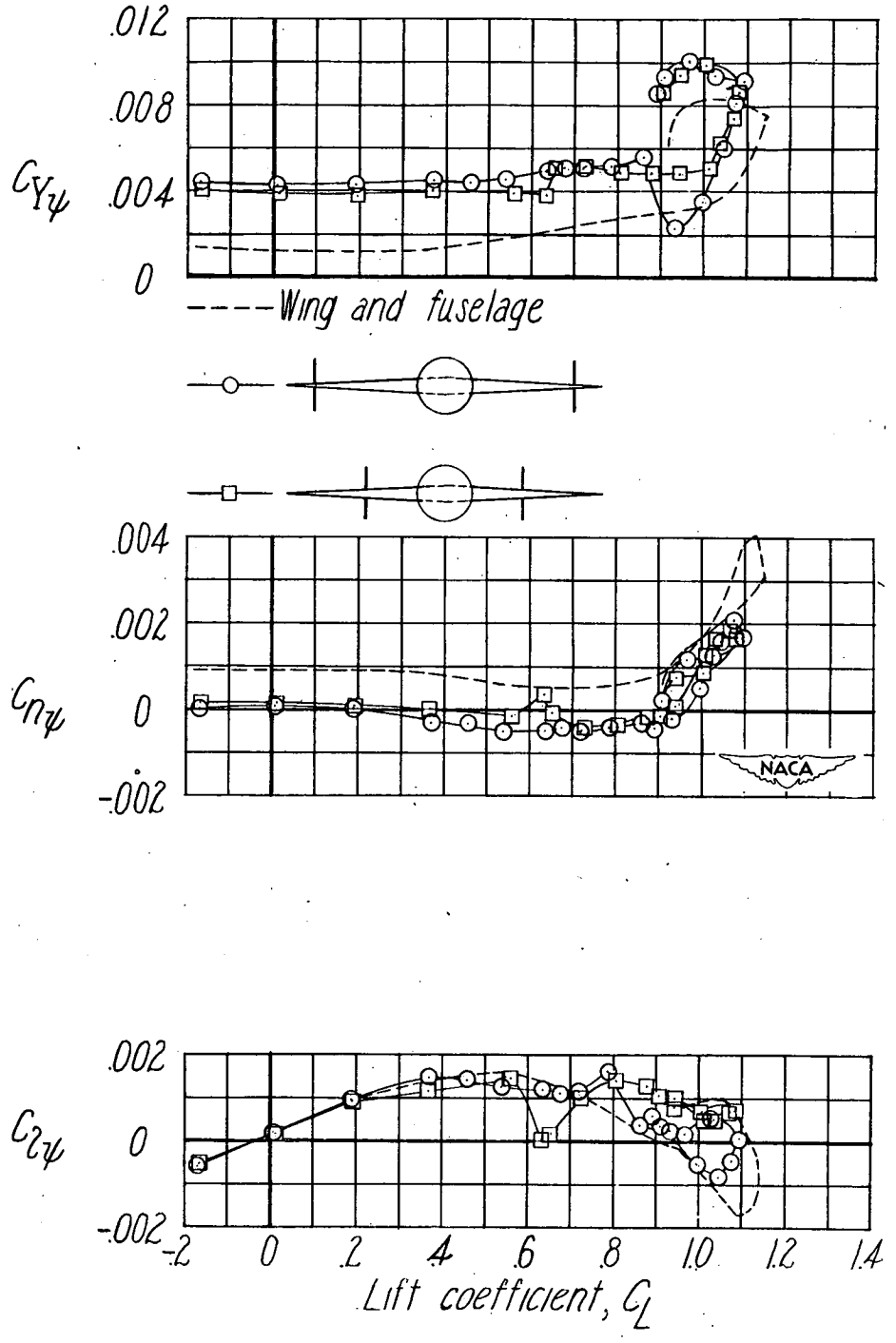

Figure 17.– Effect of outboard fin position on C_{Y_ψ}, C_{n_ψ}, and C_{l_ψ} of a triangular-wing model. Fin aspect ratio, 1.5; $\Lambda_{LE} = 45^\circ$; $\lambda = 0.45$; $\frac{S_t}{S_w} = 0.083$.

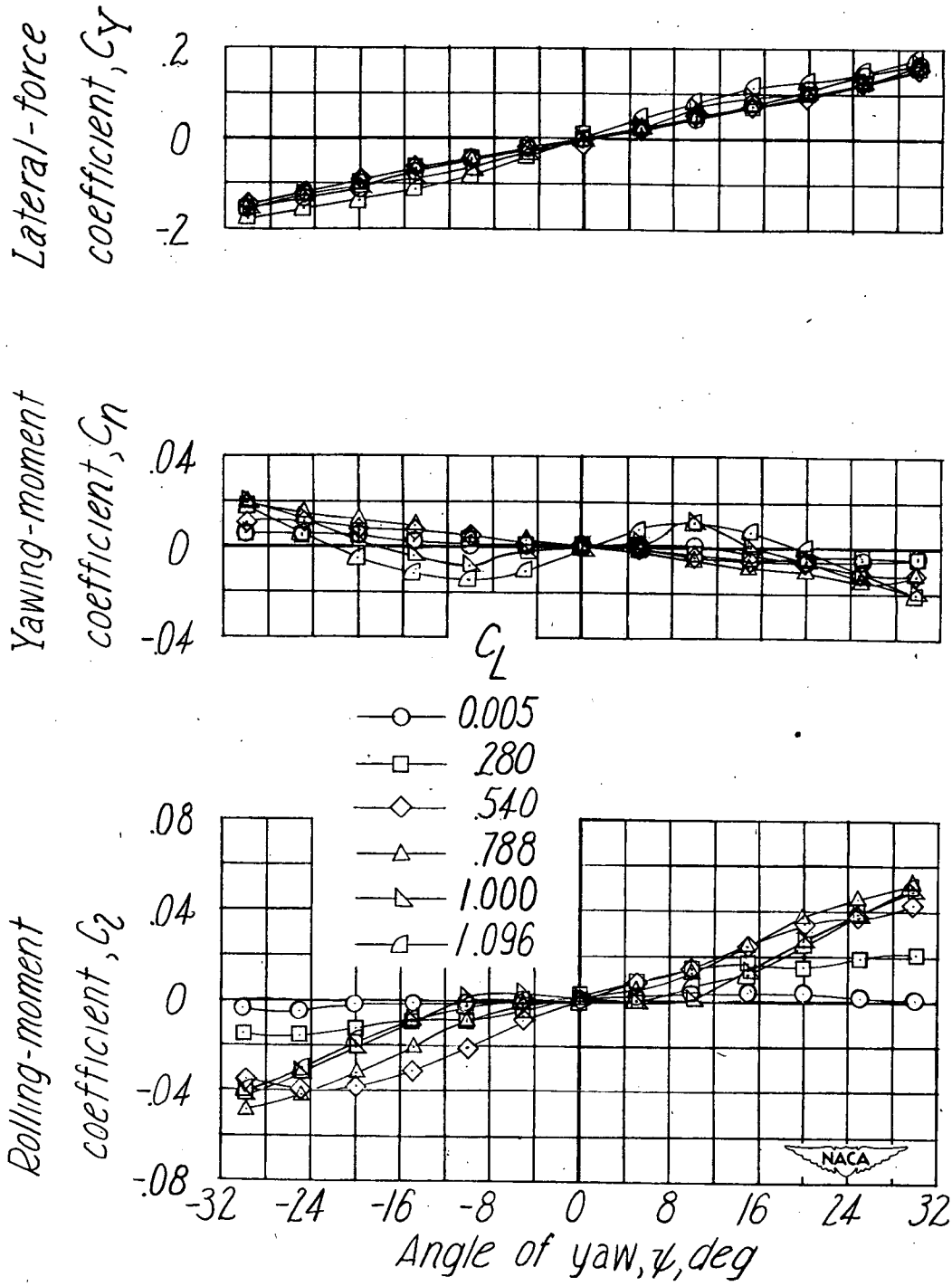

Figure 18.– Variation of C_Y, C_n, and C_l with ψ at several lift coefficients for a triangular-wing model with outboard fins in position 1. Fin aspect ratio, 1.5; $\Lambda_{LE} = 45^\circ$; $\lambda = 0.45$; $\frac{S_t}{S_w} = 0.083$.

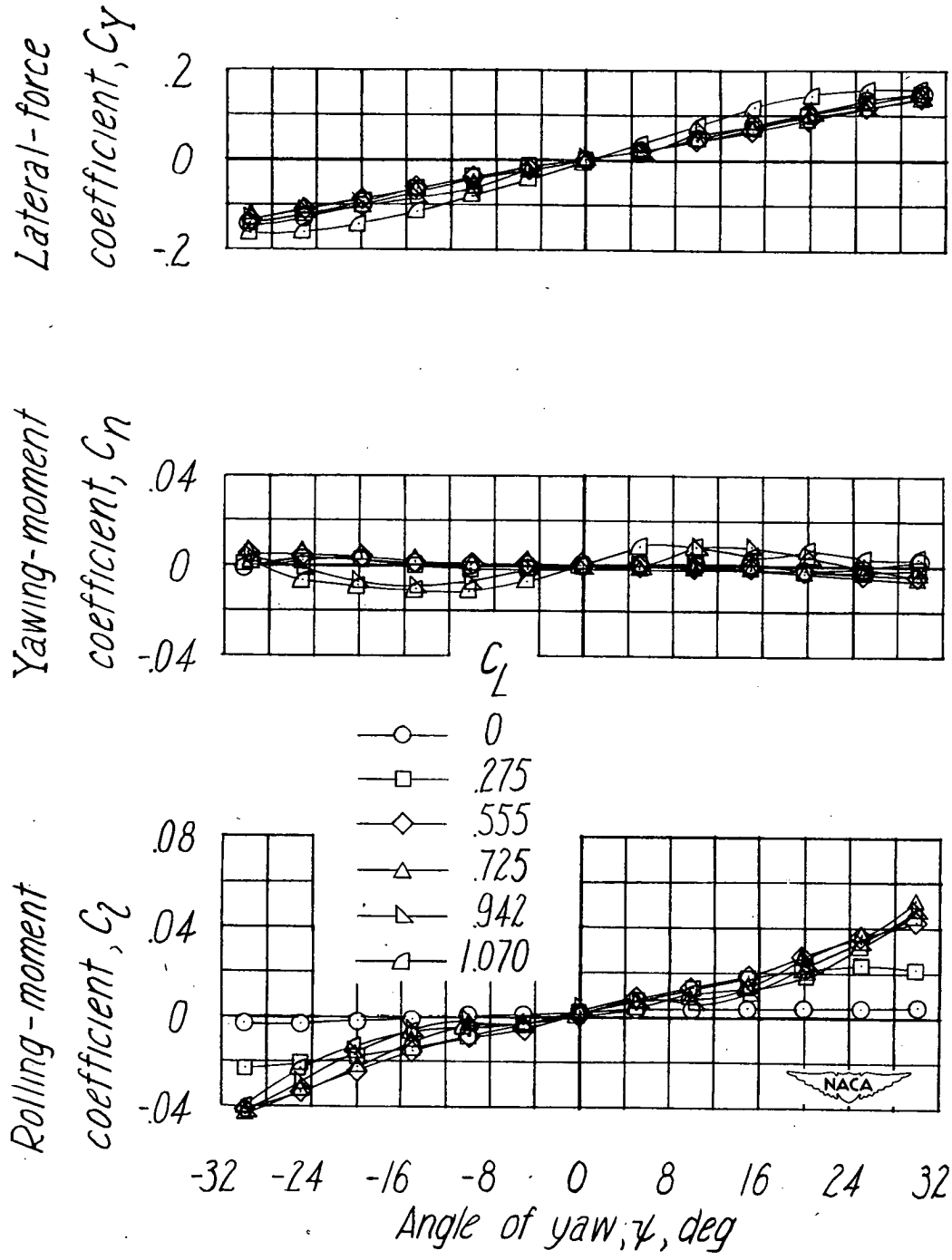

Figure 19.– Variation of C_Y, C_n, and C_l with ψ at several lift coefficients for a triangular-wing model with outboard fins in position 2. Fin aspect ratio, 1.5; $\Lambda_{LE} = 45°$; $\lambda = 0.45$; $\frac{S_t}{S_w} = 0.083$.

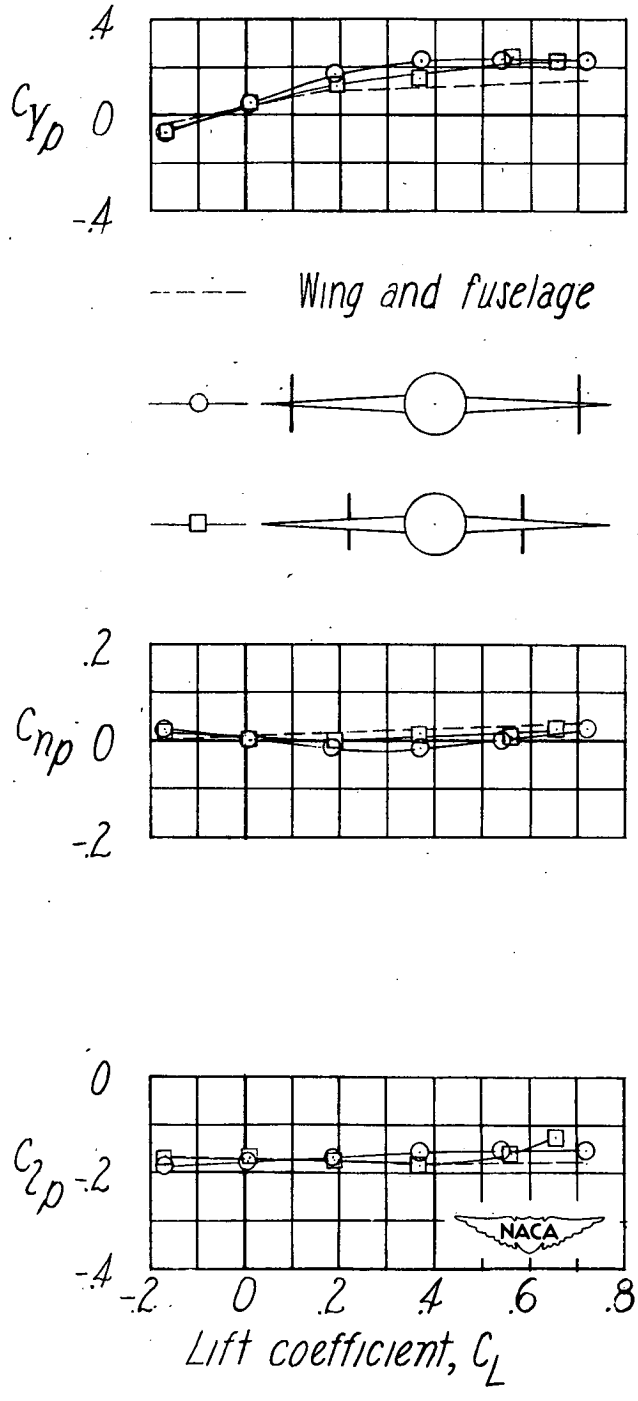

Figure 20.— Effect of outboard fin position on C_{Y_p}, C_{n_p}, and C_{l_p} of a triangular-wing model. Fin aspect ratio, 1.5; $\Lambda_{LE} = 45°$; $\lambda = 0.45$; $\frac{S_t}{S_w} = 0.083$.

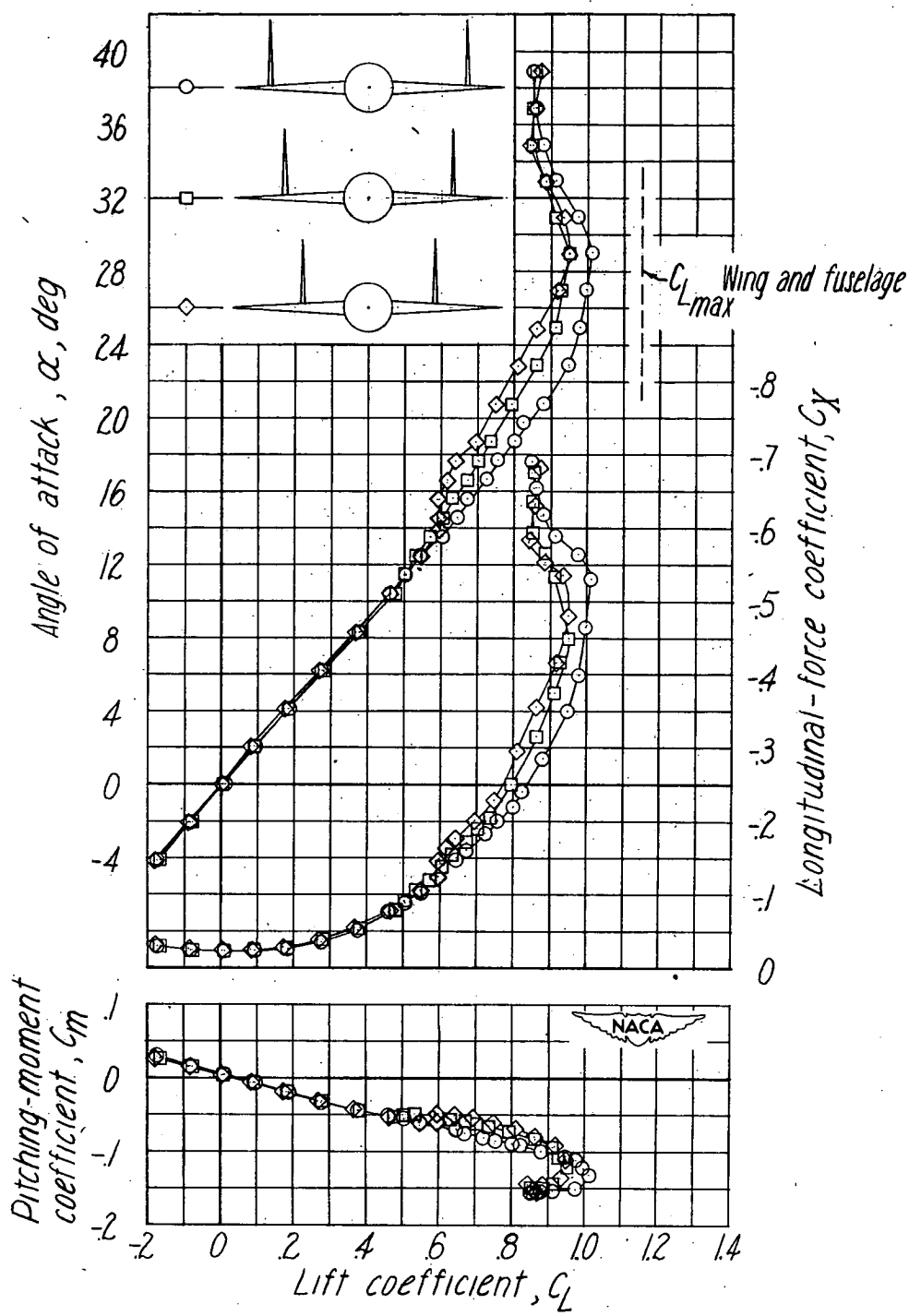

Figure 21.– Effect of outboard fin position on aerodynamic characteristics of a triangular-wing model. Fin aspect ratio, 1.4; $\Lambda_{LE} = 53^\circ$; $\lambda = 0.22$; $\frac{S_t}{S_w} = 0.22$.

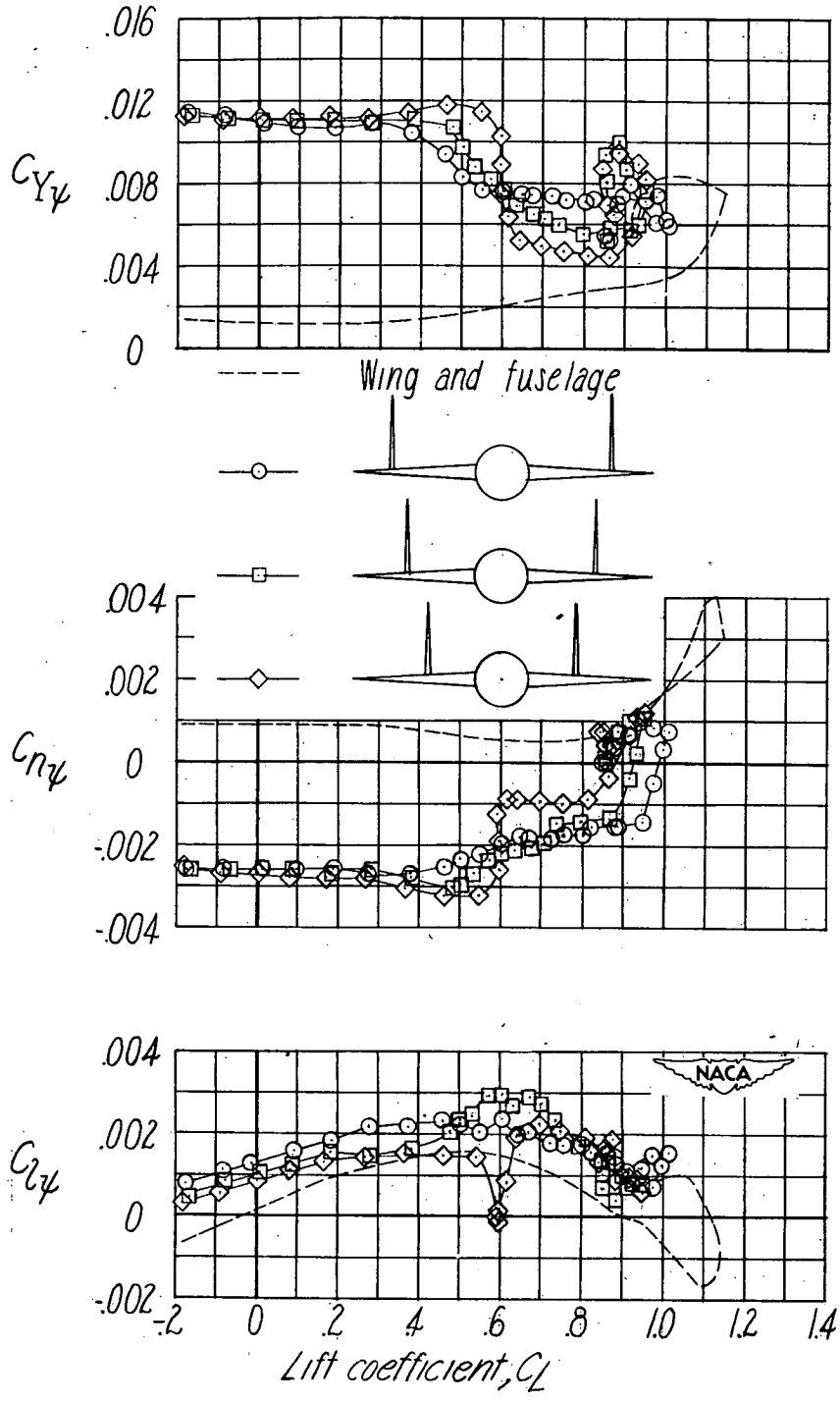

Figure 22.– Effect of outboard fin position on C_{Y_ψ}, C_{n_ψ}, and C_{l_ψ} of a triangular-wing model. Fin aspect ratio, 1.4; $\Lambda_{LE} = 53^\circ$; $\lambda = 0.22$; $\frac{S_t}{S_w} = 0.22$.

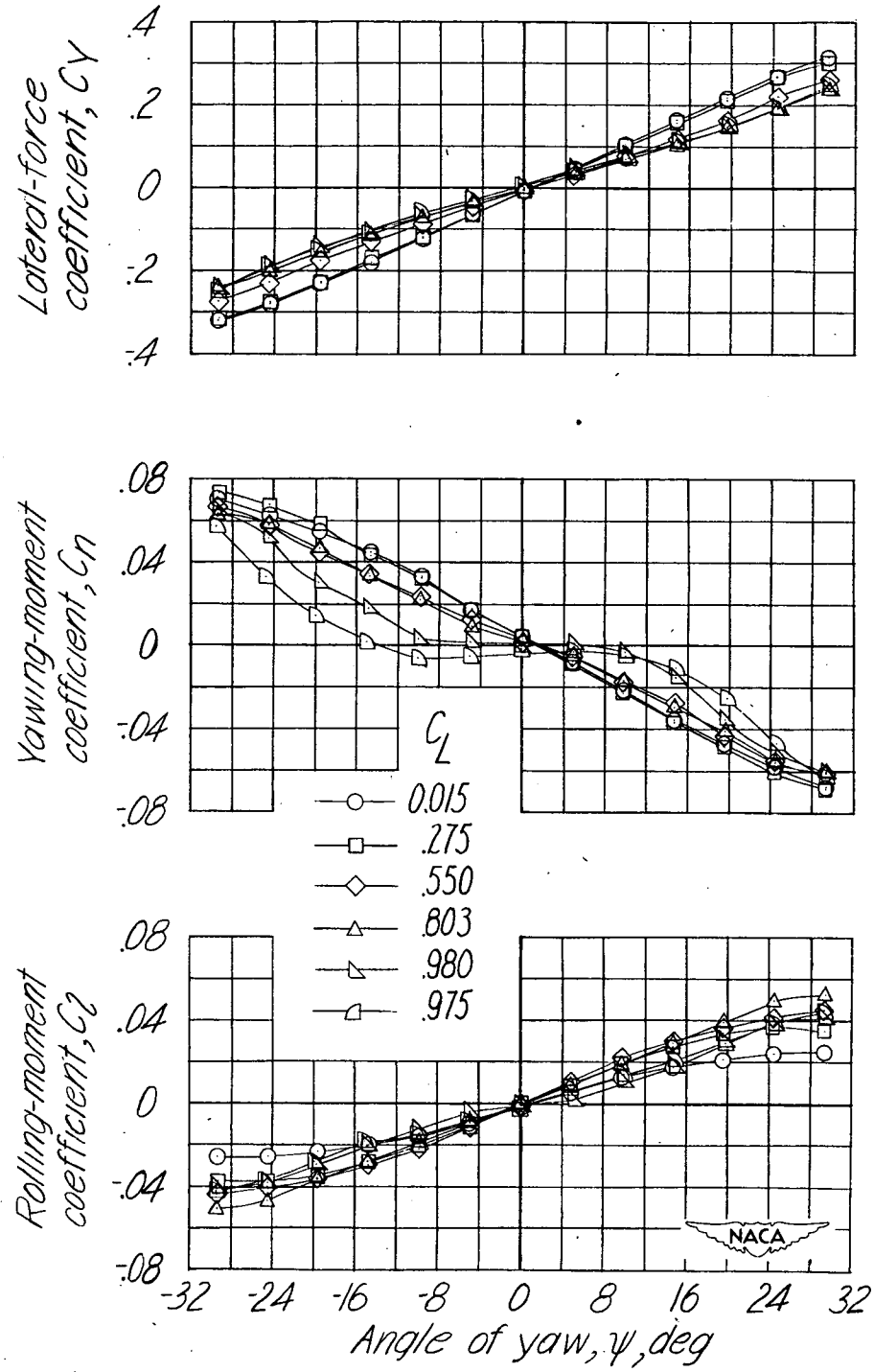

Figure 23.– Variation of C_Y, C_n, and C_l with ψ at several lift coefficients for a triangular-wing model with outboard fins in position 1. Fin aspect ratio, 1.4; $\Lambda_{LE} = 53^\circ$; $\lambda = 0.22$; $\frac{S_t}{S_w} = 0.22$.

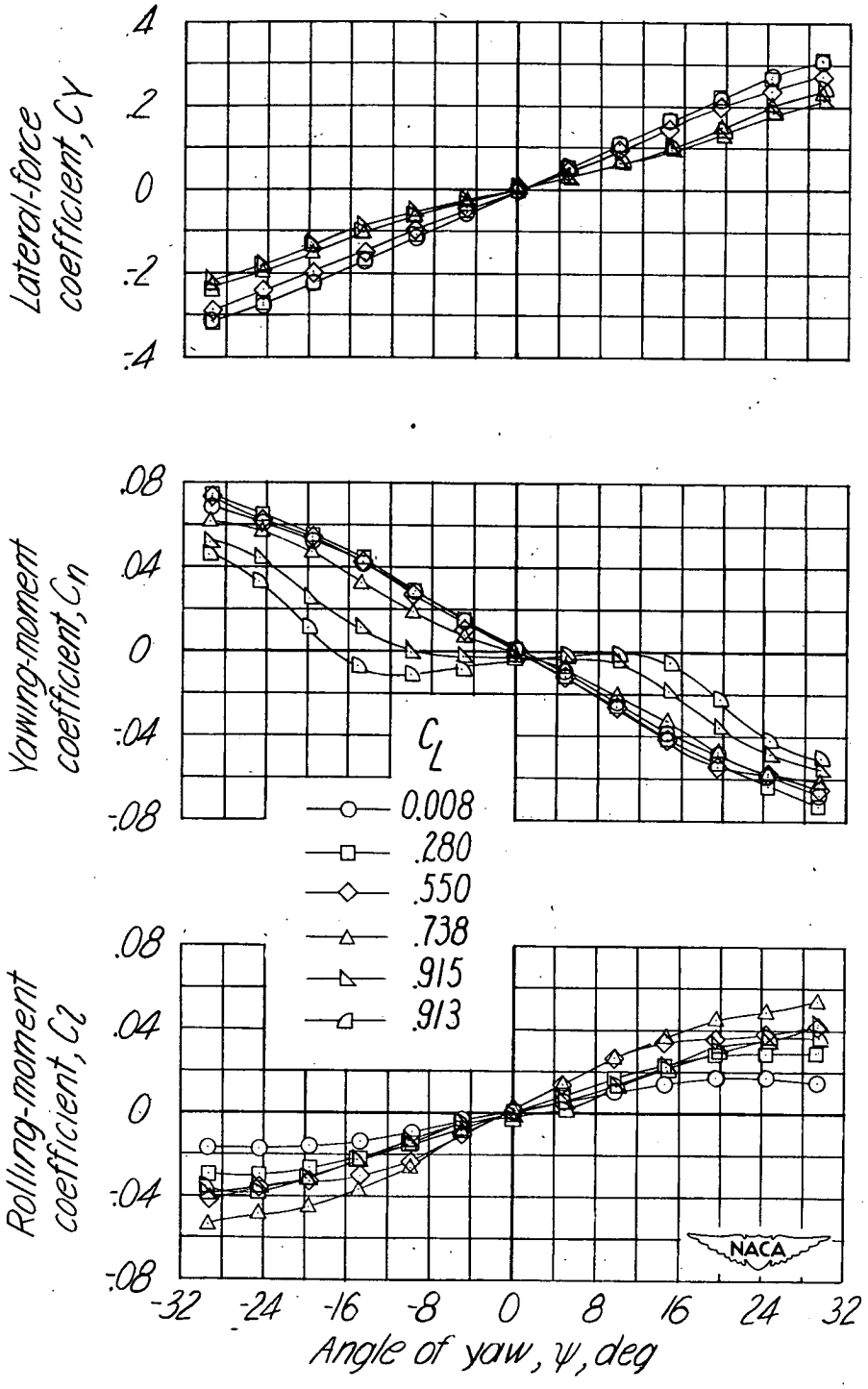

Figure 24.– Variation of C_Y, C_n, and C_l with ψ at several lift coefficients for a triangular-wing model with outboard fins in position 2. Fin aspect ratio, 1.4; $\Lambda_{LE} = 53^\circ$; $\lambda = 0.22$; $\frac{S_t}{S_w} = 0.22$.

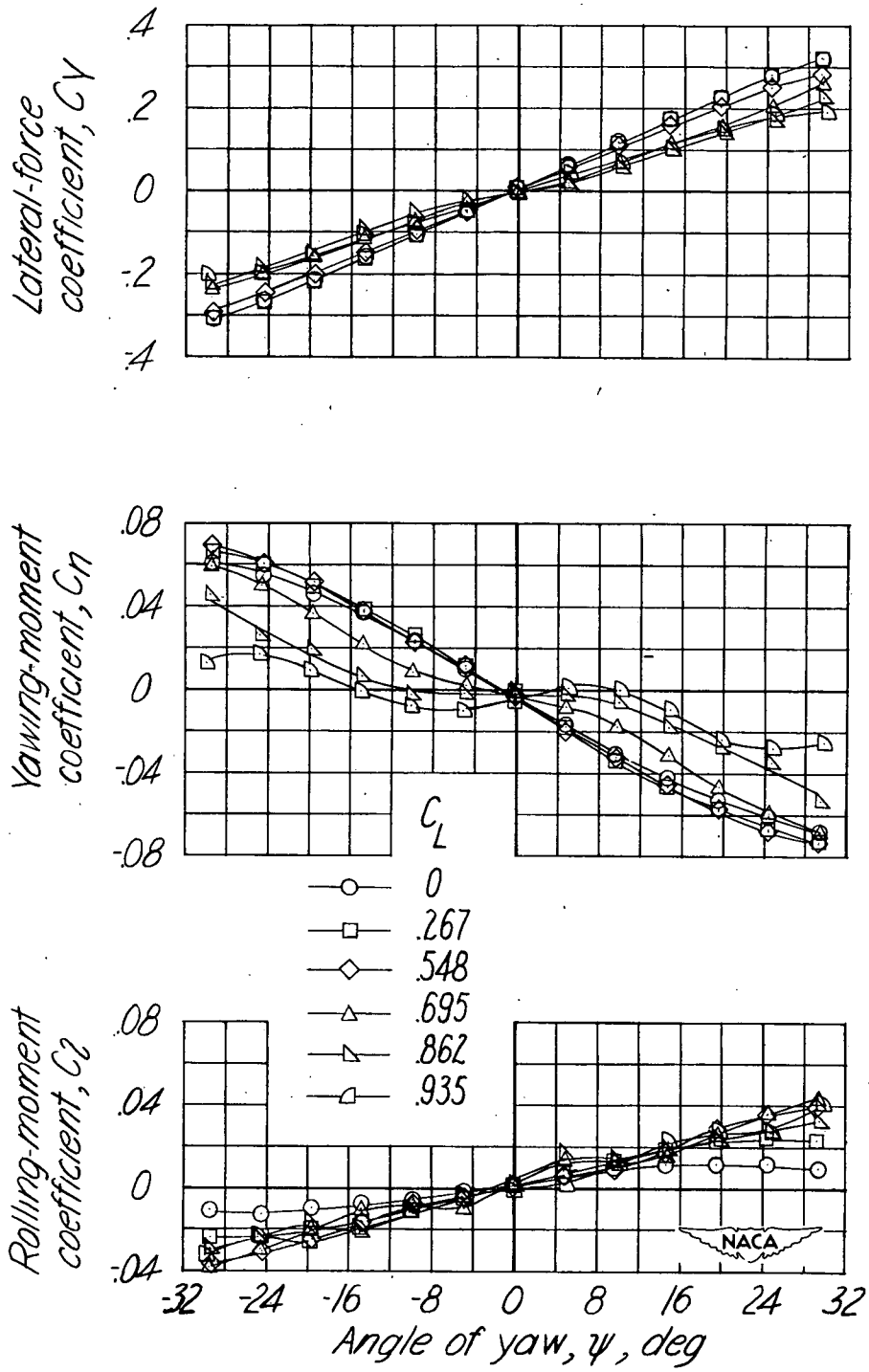

Figure 25.– Variation of C_Y, C_n, and C_l with ψ at several lift coefficients for a triangular-wing model with outboard fins in position 3. Fin aspect ratio, 1.4; $\Lambda_{LE} = 53°$; $\lambda = 0.22$; $\frac{S_t}{S_w} = 0.22$.

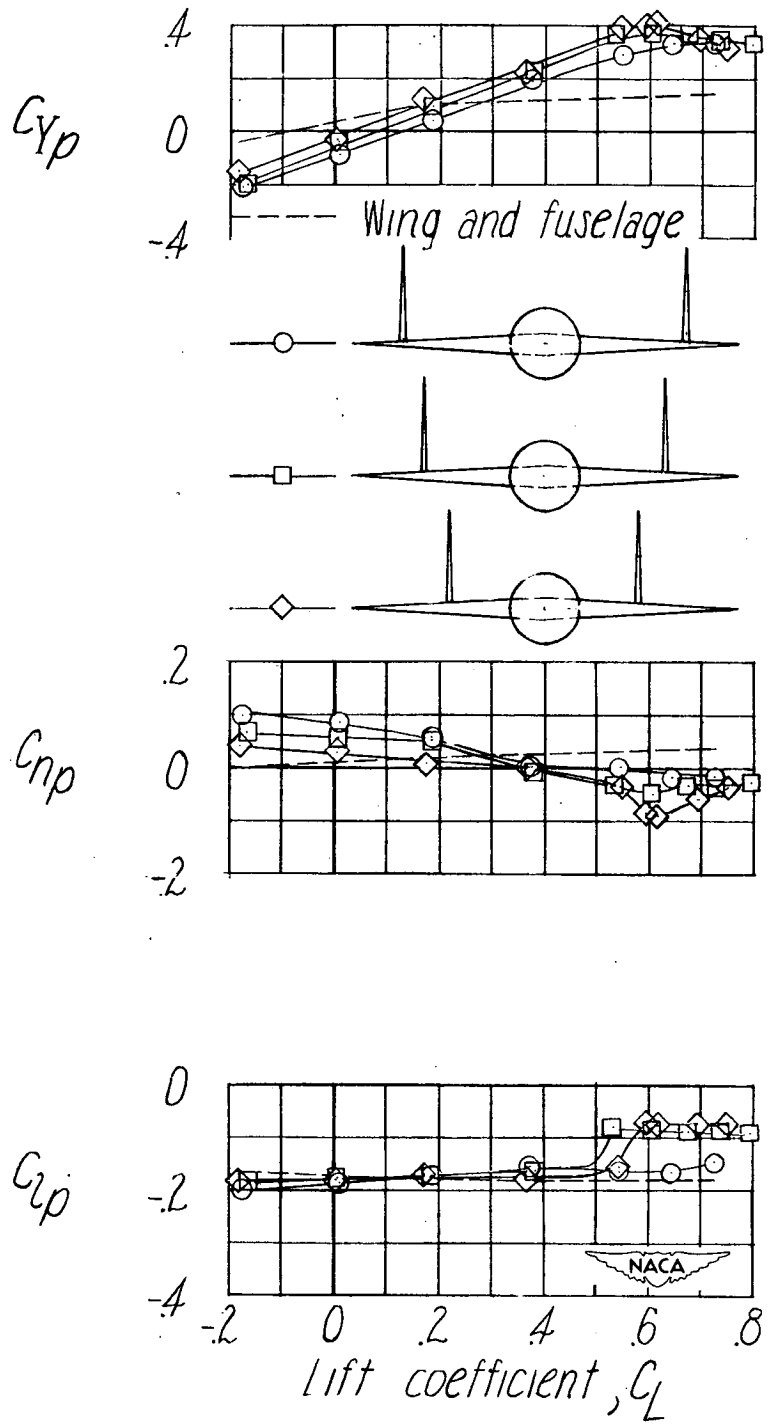

Figure 26.– Effect of outboard fin position on C_{Y_p}, C_{n_p}, and C_{l_p} of a triangular-wing model. Fin aspect ratio, 1.4; $\Lambda_{LE} = 53°$; $\lambda = 0.22$; $\frac{S_t}{S_w} = 0.22$.

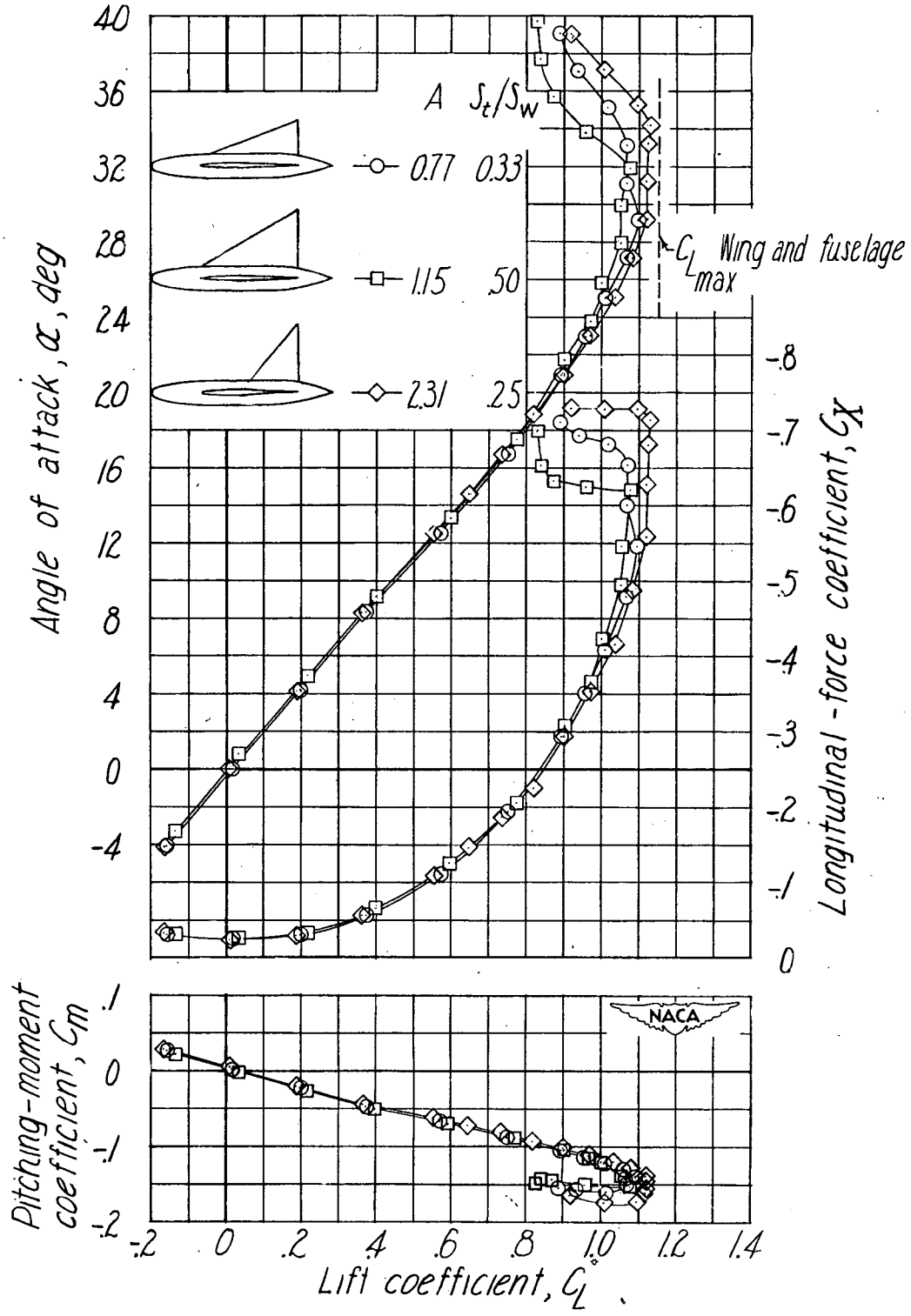

Figure 27.– Effect of central vertical fins on aerodynamic characteristics of a triangular-wing model.

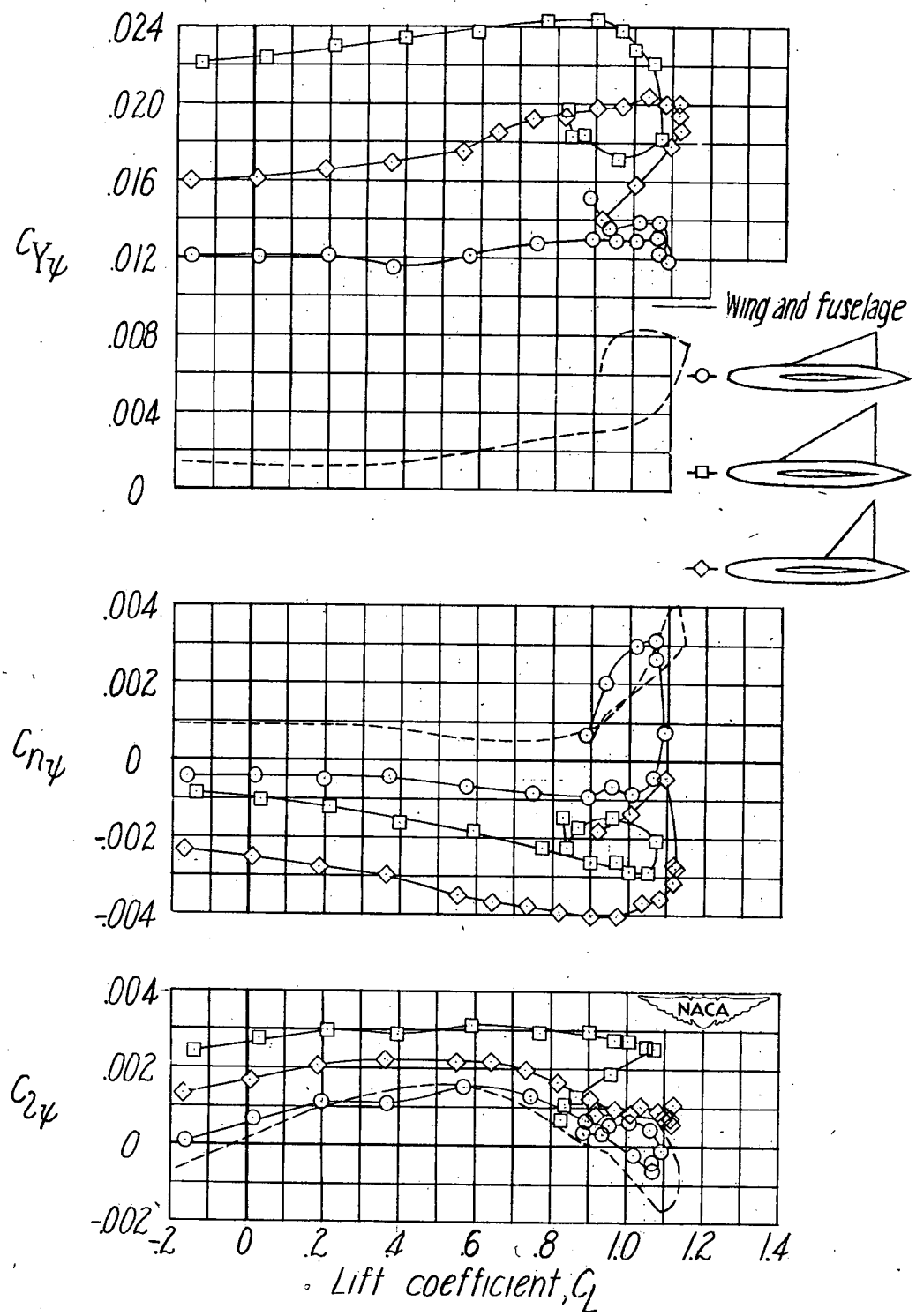

Figure 28.– Effect of central vertical fins on C_{Y_ψ}, C_{n_ψ}, and C_{l_ψ} of a triangular-wing model.

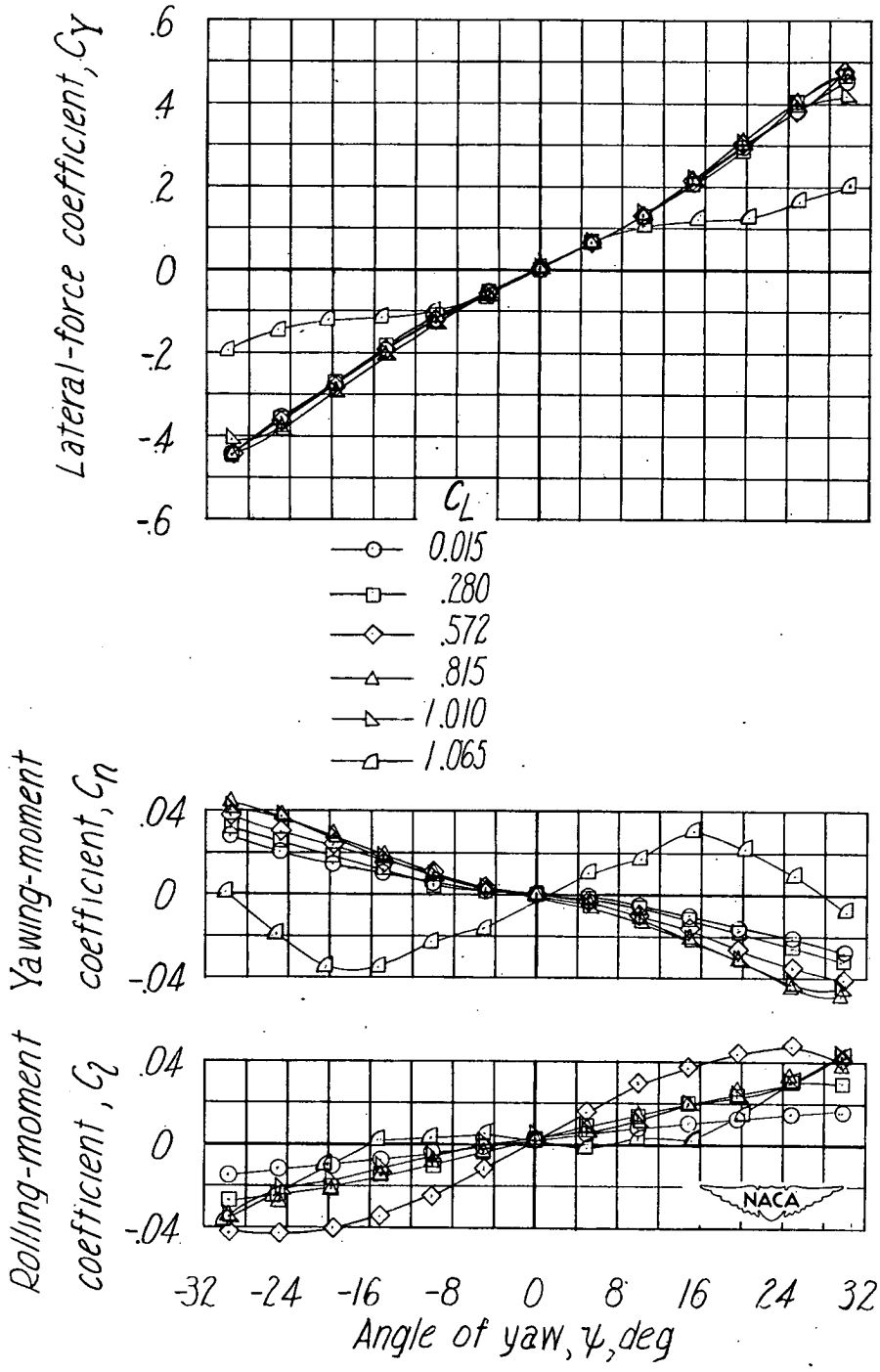

Figure 29.– Variation of C_Y, C_n, and C_l with ψ at several lift coefficients for a triangular-wing model with a fin of aspect ratio 0.77 in the forward position. $\frac{S_t}{S_w} = 0.33$.

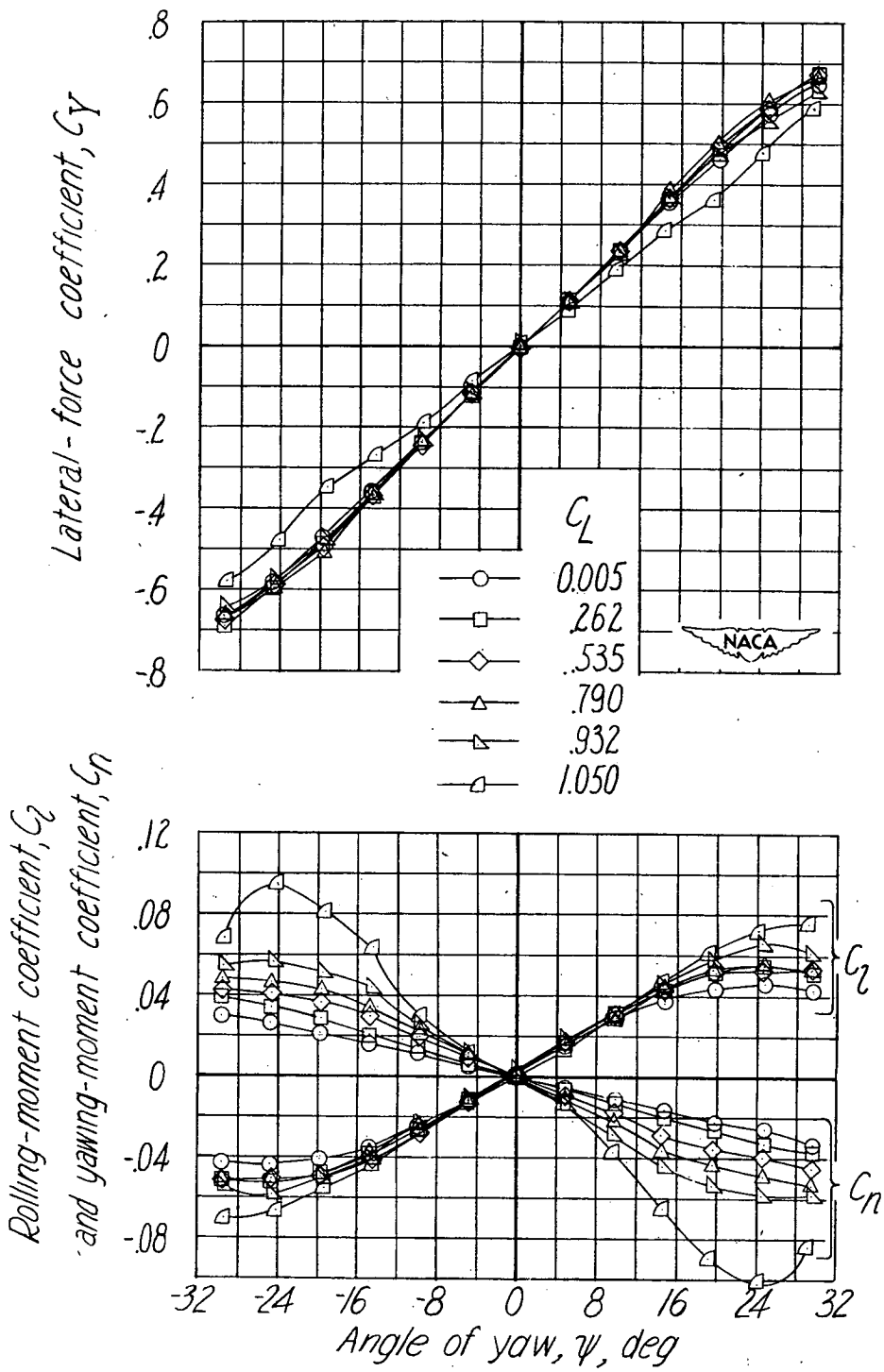

Figure 30.– Variation of C_Y, C_n, and C_l with ψ at several lift coefficients for a triangular-wing model with a fin of aspect ratio 1.15 in the forward position. $\frac{S_t}{S_w} = 0.50$.

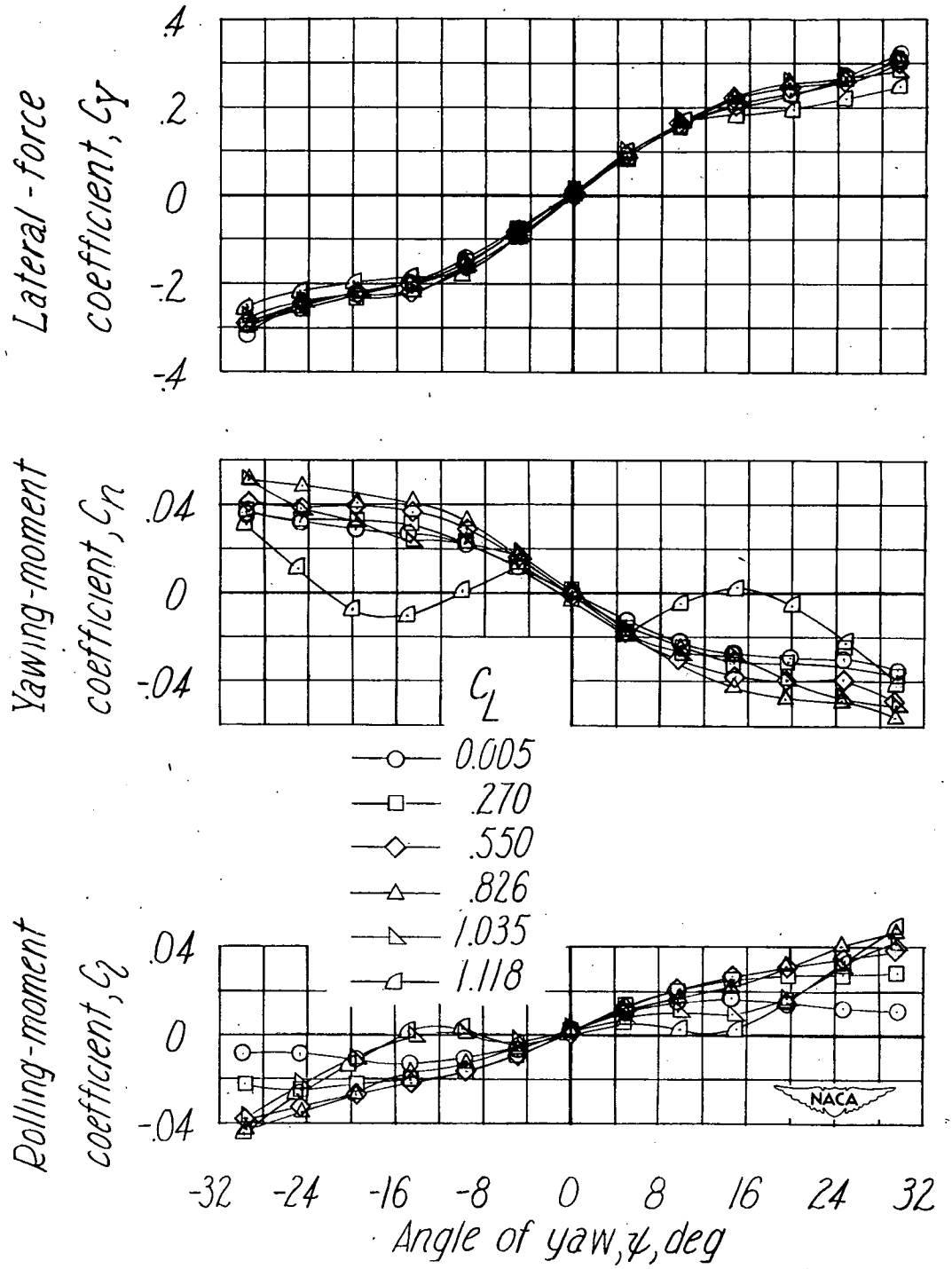

Figure 31.– Variation of C_Y, C_n, and C_l with ψ at several lift coefficients for a triangular-wing model with a fin of aspect ratio 2.31 in the forward position. $\frac{S_t}{S_w} = 0.25$.

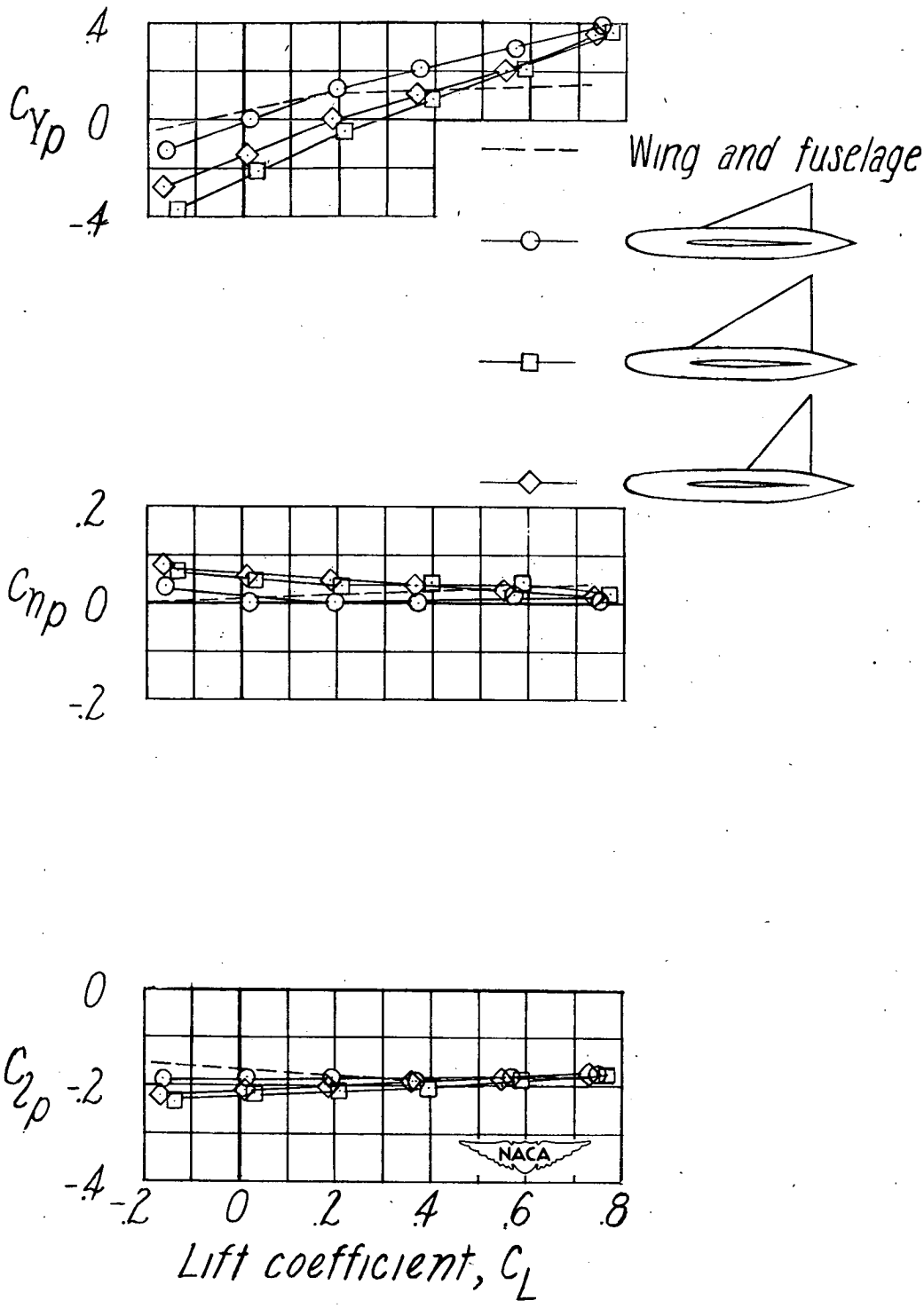

Figure 32.– Effect of central vertical fins on C_{Y_p}, C_{n_p}, and C_{l_p} of a triangular-wing model.

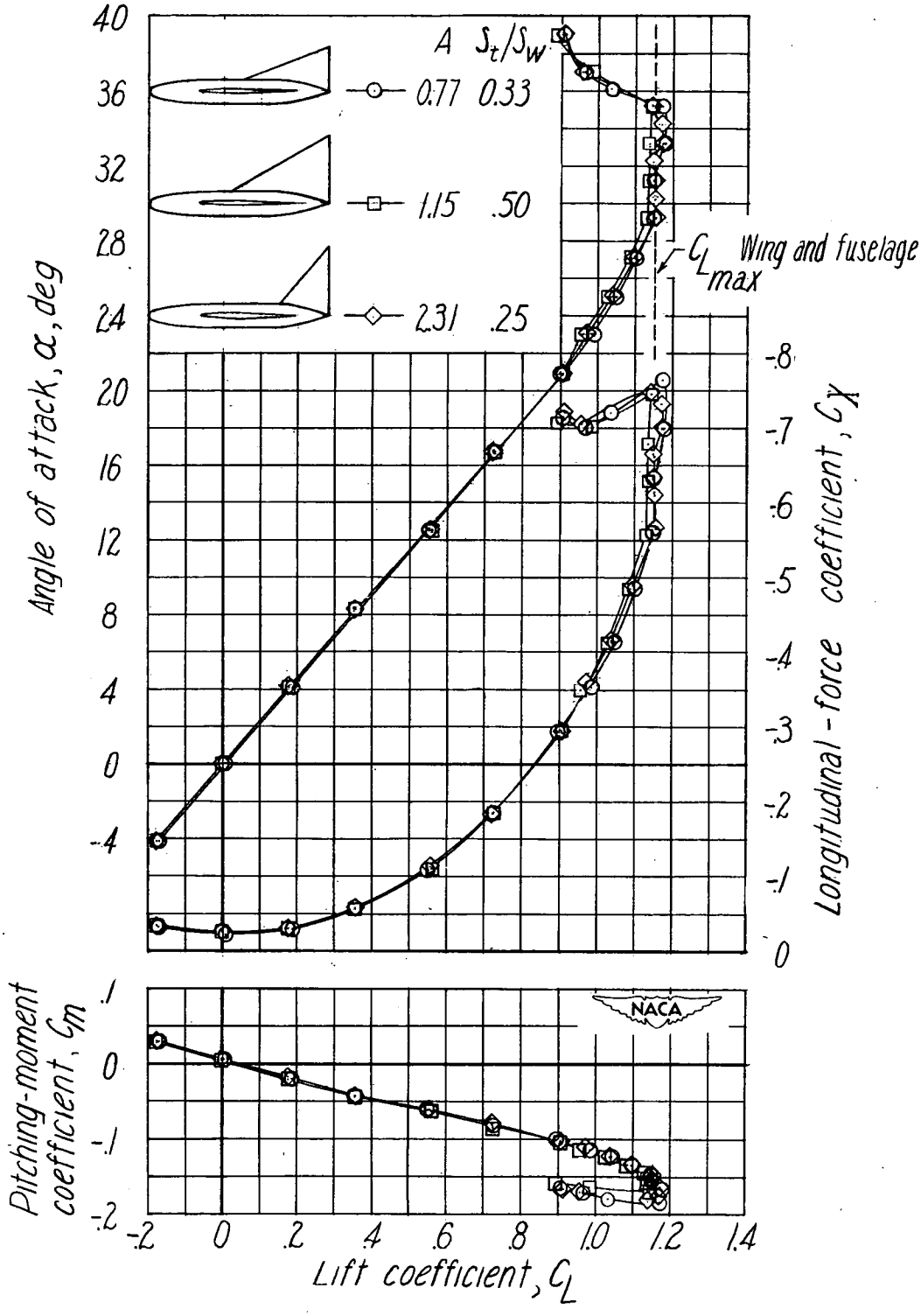

Figure 33.– Effect of central vertical fins on aerodynamic characteristics of a triangular-wing model.

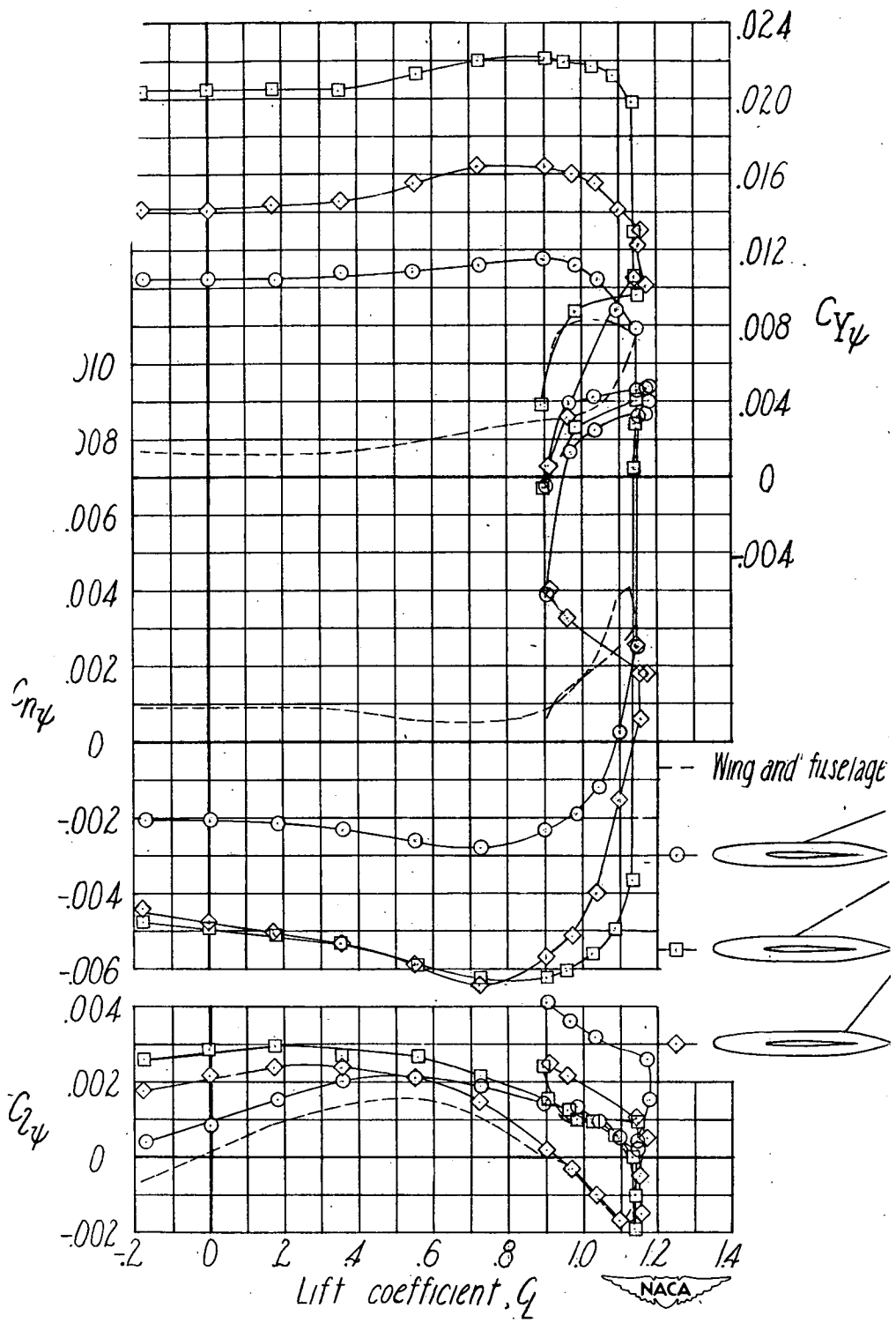

Figure 34.– Effect of central vertical fins on C_{Y_ψ}, C_{n_ψ}, and C_{l_ψ} of a triangular-wing model.

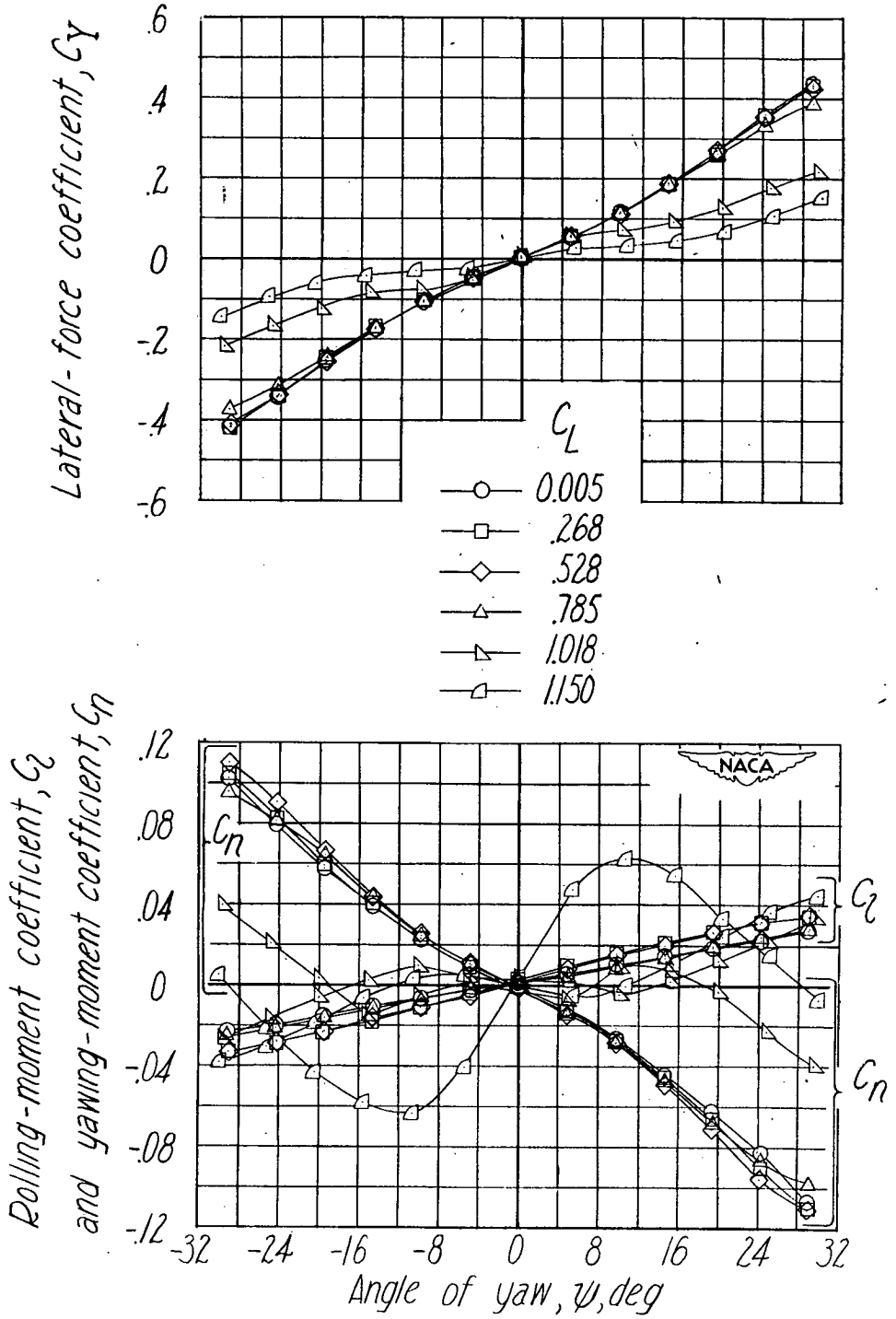

Figure 35.- Variation of C_Y, C_n, and C_l with ψ at several lift coefficients for a triangular-wing model with a fin of aspect ratio 0.77 in the rearward position. $\frac{S_t}{S_w} = 0.33$.

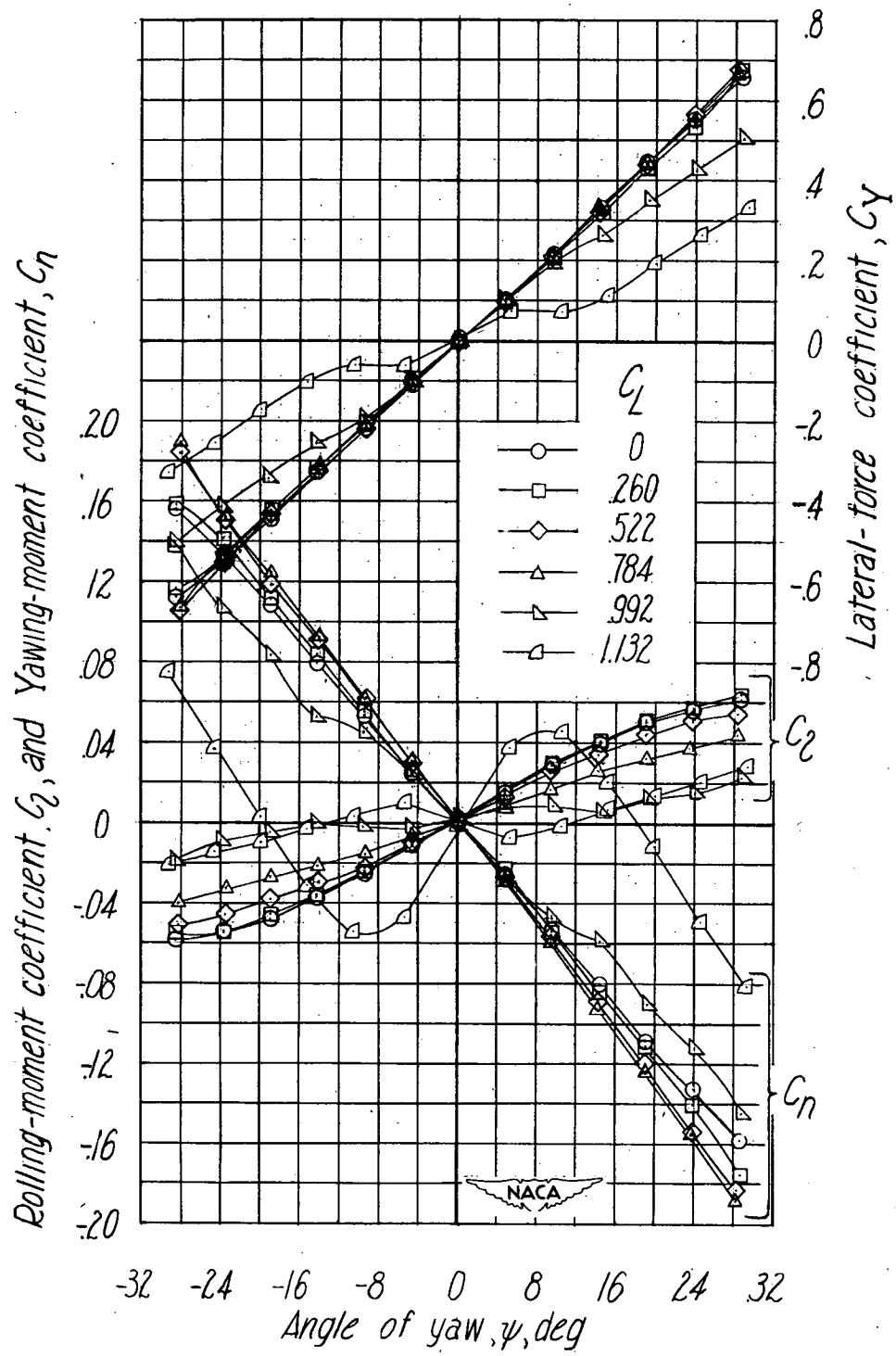

Figure 36.— Variation of C_Y, C_n, and C_l with Ψ at several lift coefficients for a triangular-wing model with a fin of aspect ratio 1.15 in the rearward position. $\frac{S_t}{S_w} = 0.50$.

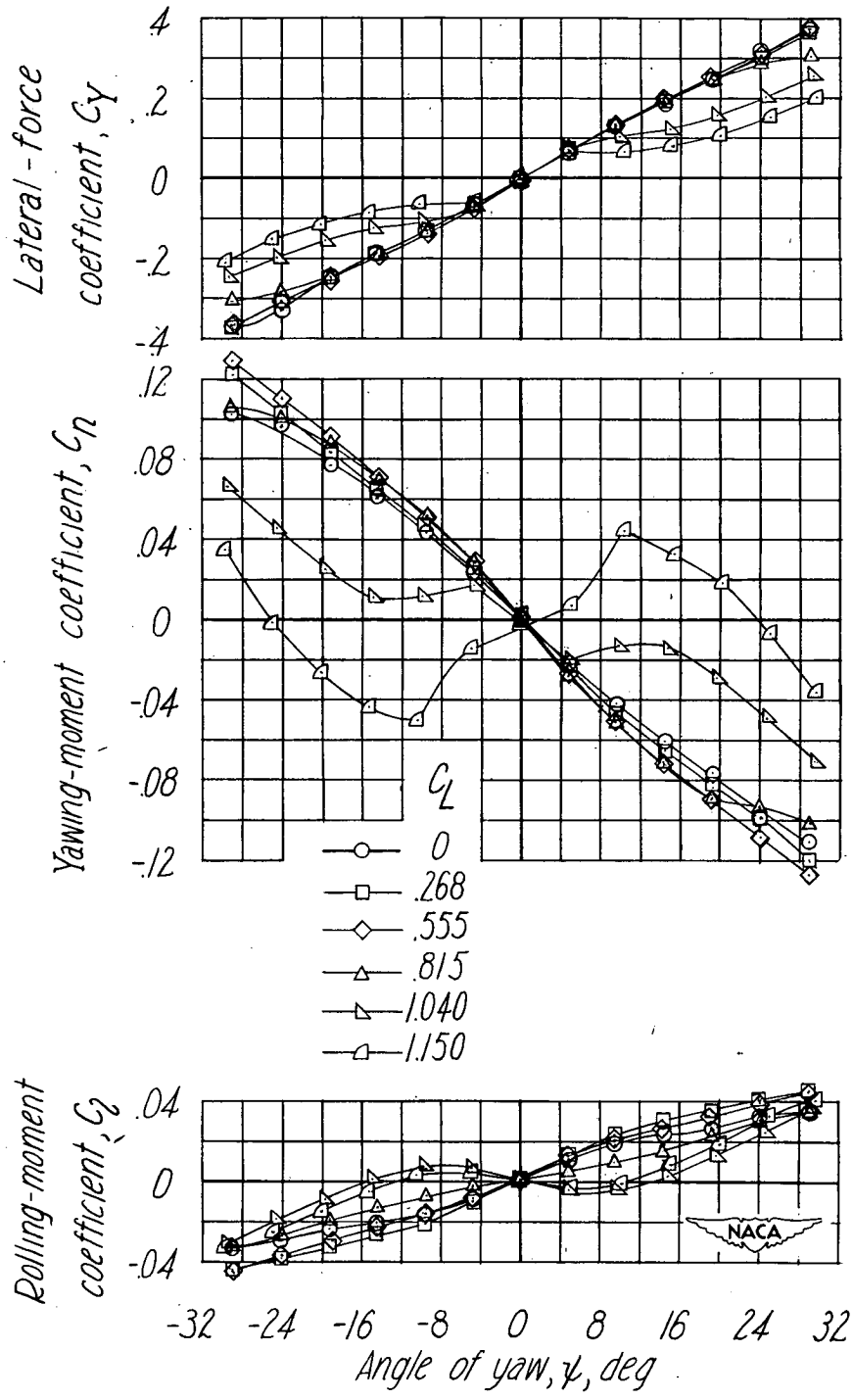

Figure 37.– Variation of C_Y, C_n, and C_l with ψ at several lift coefficients for a triangular-wing model with a fin of aspect ratio 2.31 in the rearward position. $\frac{S_t}{S_w} = 0.25$.

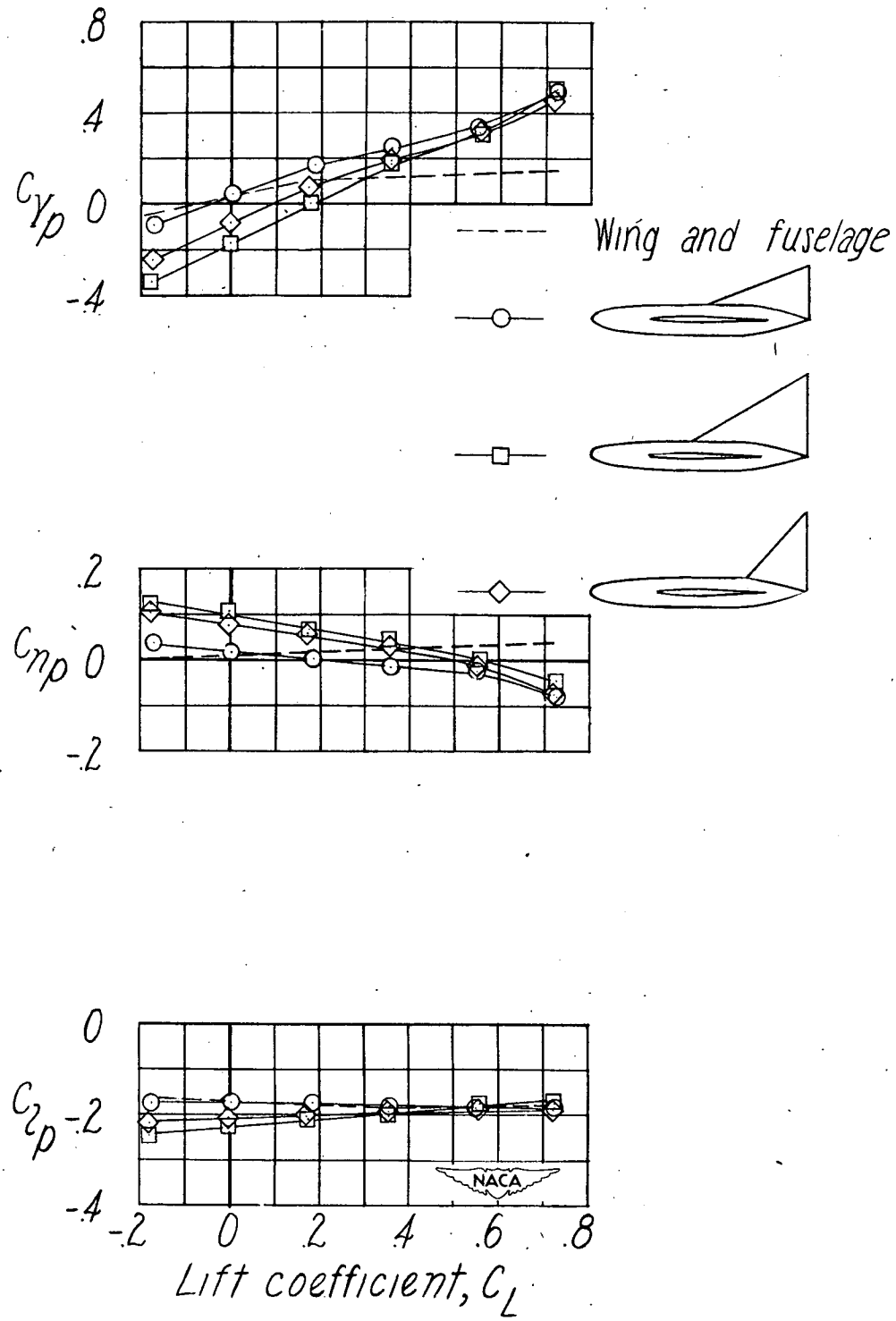

Figure 38.– Effect of central vertical fins on C_{Y_p}, C_{n_p}, and C_{l_p} of a triangular-wing model.